DOI: 10.1534/genetics.107.071803

Suppressors of *zyg-1* Define Regulators of Centrosome Duplication and Nuclear Association in *Caenorhabditis elegans*

Catherine A. Kemp,[1] Mi Hye Song,[1] Murali Krishna Addepalli,[2] Ginger Hunter and Kevin O'Connell[3]

Laboratory of Biochemistry and Genetics, National Institute of Diabetes and Digestive and Kidney Diseases, National Institutes of Health, Bethesda, Maryland 20892

Manuscript received February 6, 2007
Accepted for publication February 26, 2007

ABSTRACT

In *Caenorhabditis elegans*, the kinase ZYG-1 is required for centrosome duplication. To identify factors that interact with ZYG-1, we used a classical genetic approach and identified 21 *szy* (***s**uppressor of **zy**g-1*) genes that when mutated restore partial viability to a *zyg-1* mutant. None of the suppressors render animals completely independent of *zyg-1* activity and analysis of a subset of the suppressors indicates that all restore the normal process of centrosome duplication to *zyg-1* mutants. Thirteen of these suppressor mutations confer phenotypes of their own and cytological examination reveals that these genes function in a variety of cellular processes including cell cycle timing, microtubule organization, cytokinesis, chromosome segregation, and centrosome morphology. Interestingly, several of the *szy* genes play a role in attaching the centrosome to the nuclear envelope. We have found that one such *szy* gene is *sun-1*, a gene encoding a nuclear envelope component. We further show that the role of SUN-1 in centrosome duplication is distinct from its role in attachment. Our approach has thus identified numerous candidate regulators of centrosome duplication and uncovered an unanticipated regulatory mechanism involving factors that tether the centrosome to the nucleus.

TO accomplish its various tasks, the microtubule cytoskeleton is constantly reorganized throughout the cell cycle. In mitosis, microtubules are assembled into a bipolar spindle to segregate chromosomes and position the cytokinetic furrow. In interphase they are organized into a radial array that participates in the trafficking of material along the cell's central-peripheral axes. This reorganization is largely under control of the centrosome, the cell's primary microtubule-organizing center. Through its capacity to nucleate and anchor microtubules, the centrosome organizes the radial arrays of interphase cells and the poles of the mitotic spindle (Doxsey 2001).

The morphology of the animal centrosome varies somewhat among species but overall its basic structure is conserved (Azimzadeh and Bornens 2004). It is composed of two parts: an orthogonally aligned pair of centrioles and an associated matrix of pericentriolar material (PCM). Centrioles are cylindrical structures composed of a ninefold symmetric arrangement of microtubules and are important for maintaining a discrete domain of PCM (Bobinnec *et al.* 1998). Each centrosome contains one "mother" centriole that is at least one cell cycle old and one "daughter" centriole synthesized during the last round of centrosome duplication. The PCM is the site of microtubule nucleation and anchoring. Although its exact molecular composition and structural organization are not known, it contains a high concentration of coiled-coil domain proteins that are thought to provide a scaffold for anchoring the γ-tubulin ring complexes that nucleate microtubules (Doxsey 2001).

Unlike other organelles, the centrosome is not membrane bound but it does maintain a close association with the nuclear envelope. Recently, three proteins have been identified that play a key role in maintaining this close association. Loss of ZYG-12, a *Caenorhabditis elegans* member of the Hook family of cytoskeletal linker proteins, results in detachment of the centrosome from the nucleus (Malone *et al.* 2003). Such mutants exhibit spindle defects, chromosome missegregation, and lethality, indicating that at least in the *C. elegans* embryo, association of the centrosome and nucleus is essential. ZYG-12 localizes to both the nuclear envelope and centrosomes and is thought to maintain anchorage through self-association. ZYG-12 also physically interacts with cytoplasmic dynein (Malone *et al.* 2003) and loss of dynein activity results in a detached centrosome phenotype (Gonczy *et al.* 1999a; Yoder and Han 2001).

[1]These authors contributed equally to this work.

[2]*Present address:* Reliance Life Sciences, Navi Mumbai 400 701, India.

[3]*Corresponding author:* Laboratory of Biochemistry and Genetics, National Institute of Diabetes and Digestive and Kidney Diseases, National Institutes of Health, 8 Center Dr., Room 2A07, Bethesda, MD 20892. E-mail: kevino@intra.niddk.nih.gov

Finally, another conserved component of the nuclear envelope, SUN-1, is required for centrosome–nuclear association. SUN-1, a member of a family of proteins characterized by the presence of a membrane-spanning region and a C-terminal SUN domain (Starr and Fischer 2005), is required for nuclear localization of ZYG-12 (Malone *et al.* 2003).

Like DNA, centrosomes duplicate precisely once per cell cycle during S phase. Ultrastructural studies have resolved duplication into a few discrete steps (Sluder 2004). The first step involves the separation of mother and daughter centrioles, which move a short distance apart, losing their orthogonal orientation. Centriole synthesis then initiates with the formation of a precursor, or procentriole, next to and at a right angle to each preexisting centriole. Finally, the procentrioles elongate to form complete daughter centrioles. The two resulting centriole pairs ultimately migrate apart. As the cell approaches mitosis, each centrosome "matures" as it accumulates PCM and acquires increased microtubule-nucleating capacity.

Defects in centrosome duplication can result in spindles with an abnormal number of poles. For instance, monopolar spindles can result from duplication failure while multipolar spindles can result from a failure to limit centrosome duplication to one round per cell cycle. Interestingly, many tumor cells contain more than two centrosomes, suggesting that errors in centrosome duplication contribute to genomic instability and cancer (Sankaran and Parvin 2006). Despite the obvious importance of centrosome duplication, little is known about the molecular events that compose this process. In addition, how duplication is limited to one round per cell cycle and how it is temporally coordinated with other cell cycle events are still not well understood.

Work in a variety of organisms over the past decade has led to an expanding inventory of proteins that function in this process. In particular, genetic analysis in *C. elegans* has led to the identification of five core components of the duplication machinery. These include the kinase ZYG-1 (O'Connell *et al.* 2001) and four coiled-coil domain-containing proteins: SPD-2, SAS-4, SAS-5, and SAS-6 (Kirkham *et al.* 2003; Leidel and Gonczy 2003; Dammermann *et al.* 2004; Delattre *et al.* 2004; Kemp *et al.* 2004; Pelletier *et al.* 2004; Leidel *et al.* 2005). Loss of any one of these factors leads to a complete block whereby mother and daughter centrioles separate but no new centrioles are formed. In addition, Dammermann *et al.* (2004) have shown that SPD-5, another coiled-coil domain protein (Hamill *et al.* 2002), and γ-tubulin also are at least partially required for centriole formation. In the case of SAS-6, a vertebrate ortholog has been identified and demonstrated to have the same function (Leidel *et al.* 2005). Potential vertebrate orthologs of SPD-2 and SAS-4 exist as well, suggesting that worms and vertebrates utilize the same basic machinery (Leidel and Gonczy 2003; Pelletier *et al.* 2004).

Despite a multitude of mutant hunts (Hirsh and Vanderslice 1976; Miwa *et al.* 1980; Cassada *et al.* 1981; Kemphues *et al.* 1988a,b; O'Connell *et al.* 1998; Gonczy *et al.* 1999b) and exhaustive genomewide RNAi-based screening (Kamath *et al.* 2003; Simmer *et al.* 2003; Sonnichsen *et al.* 2005), no additional factors have been implicated in centrosome duplication. It is thus unlikely that existing forward and reverse genetic screening strategies will be very effective in identifying many more genes with important roles in this process. Therefore, a more focused screening strategy is needed. One such strategy is a genetic modifier screen whereby one screens for mutations that enhance or suppress the phenotype of an existing mutant. Genes whose products interact in either a positive or a negative manner with the gene of interest can thus be identified. For lethal mutations, the suppressor screen is particularly powerful as it allows one to rapidly and efficiently select for mutations that restore some degree of viability.

Here we have devised a highly sensitive version of the suppressor screen to identify mutations that restore viability to strains carrying a lethal mutation. The design of the screen is such that it can be performed on any scale to rapidly and efficiently identify suppressor mutations of high or low potency, including those suppressor mutations that are deleterious. We have applied this approach to identify suppressor mutations that restore centrosome duplication to a strain compromised for *zyg-1* function and have identified 40 independent suppressor mutations that define 21 genes. Many of these genes appear to encode factors with essential functions. Unexpectedly, we identified one of these suppressors as a loss-of-function allele of the *sun-1* gene. RNAi of *sun-1* in a *zyg-1* mutant strain also restores centrosome duplication whereas RNAi of *zyg-12* does not, indicating that SUN-1 regulates centrosome duplication independently of its role in centrosome–nuclear attachment. Thus, our approach has identified a large number of candidate regulators of the centrosome duplication pathway and has uncovered an unexpected SUN-1-dependent regulatory pathway.

MATERIALS AND METHODS

Worm strains and culture conditions: Nematode strains carrying the following markers were derived from the wild-type Bristol strain N2: LGI, *dpy-5(e61) unc-13(e1091)*; LGII, *lin-31(n301)*, *dpy-25(e817)*, *zyg-1(it25)*, *zyg-1(or409)*, *bli-2(e768)*, *dpy-10 (e128)*, *unc-4(e120)*, and *unc-53(n569)*; LGIII, *unc-93 (e1500)*, *dpy-17(e164)*, *unc-32 (e189)*, *dpy-18(e364)*, *unc-25(e156)*, and *unc-64(e246)*; LGV, *dpy-11(e224)*, *sma-1(e30)*, and *unc-76(e911)*; LGX, *daf-3(e1376)* and *lon-2(e678)*. Genetic analysis was performed using the following *gfp*-marked balancer chromosomes: *hT2*[*bli-4(e937) qIs48*] (I:III), *mIn1*[*dpy-10(e128) mIs14*] II, and *nT1*[*qIs51*] (IV;V). Each balancer chromosome was marked with the same three fusion constructs: *myo-2::gfp*, *pes-10::gfp*, and a gut enhancer fused to the *gfp* gene. An integrated *egl-15::gfp* transgene (*ayIS2 IV*) was used to mark suppressor heterozygotes, and the wild-type

Hawaiian variant CB4856 was used for single-nucleotide polymorphism (SNP) mapping.

Worms were cultured on NGM, modified Youngren's, only Bacto-peptone (MYOB) (Church *et al.* 1995), or high growth media seeded with *Escherichia coli* strain OP50. Strains were maintained at 16° or 20° and tested for suppression at 23.5°, 24°, or 25°. Incubator temperature was checked periodically with a high precision temperature probe and maintained within 0.2° of the set point. Tests for suppression were carried out with positive and negative controls and, where possible, all controls carried the same morphological markers as the test strains.

Suppressor screen: Worms were mutagenized on three separate occasions as follows. Mixed-stage cultures of *zyg-1 (it25)* II; *daf-3(e1376) lon-2(e678)* X worms were washed off plates with M9 buffer and treated in suspension with 40 mM ethyl methanesulfonate (EMS) as described by Brenner (1974). The inclusion of the *daf-3 lon-2* chromosome prevented animals from entering dauer diapause and thus allowed us to screen at high worm density. Following EMS treatment, 600 P_o L4 larvae were picked, 25 per plate, to 24 100-mm NGM plates and incubated at 16° until the majority of F_1 individuals became gravid. Each plate (or pool) was then processed individually as follows. The worms were washed off with water and transferred to a 15-ml conical tube. To determine the number of haploid genomes screened in each pool, a sample of the worm suspension was removed and the number of gravid F_1 hermaphrodites counted. From this number we estimated the total number of gravid F_1 worms and doubled the number to arrive at the number of haploid genomes. Worms were collected from the remainder of each F_1 worm suspension by centrifugation and a pool of F_2 eggs was then isolated by treating the worm suspension with 1 ml of 1% hypochlorite, 0.5 M NaOH for 5 min at room temperature in a microfuge tube. After all adults and larvae were dissolved, intact embryos, which are resistant to hypochlorite owing to the presence of an egg shell, were recovered by centrifugation at 4000 rpm for 3 min. The embryos were washed one to two times with 1 ml M9 buffer and then distributed between two 100-mm high growth plates. The embryos were allowed to hatch overnight at 16° and shifted to 24° the next day. Plates were incubated between 3 and 6 weeks and examined periodically for viable lines. To ensure independence, only one suppressor was isolated from each pool. All initial isolates were maintained at 20°, and those that grew reproducibly upon retesting at 23.5° or 24° were selected for further analysis.

Genetic analysis: Before analysis, strains were backcrossed at least twice to the original *zyg-1(it25)* line to remove any extraneous mutations produced during EMS treatment. To quantify suppression, L4 hermaphrodites from each backcrossed line were picked to individual 35-mm MYOB plates and incubated at either 23.5° or 24°. Approximately 24 hr later, hermaphrodites were removed and the plates were returned to 24°. Live (larvae) and dead (unhatched eggs) were counted the next day. For each strain, the progeny of 4–10 hermaphrodites were analyzed. In an identical manner, we tested *zyg-1(it25)* animals heterozygous for each suppressor. Suppressor heterozygotes were generated by mating suppressor-bearing *zyg-1(it25)* hermaphrodites to *zyg-1(it25); ayIs2 IV* males. Outcross L4 hermaphrodite progeny [genotype *zyg-1(it25); szy/+; ayIs2/+*] were identified on the basis of the presence of the *egl-15::gfp* marker. For *sun-1(bs12)* and *szy-20(bs52)*, we found that embryonic viability was higher during the second 24-hr period at elevated temperature. We report these values in Figure 1C and Table 1.

To assign each suppressor to a chromosome, we first tested for linkage to *zyg-1* (chromosome II) using standard genetic methodology (Brenner 1974). Suppressors that did not show linkage to *zyg-1* were mapped to one of the other chromosomes using the snip–SNP mapping technique (Wicks *et al.* 2001). To SNP map suppressors, we created OC118, a *zyg-1(it25)* Hawaiian congenic strain by backcrossing the *zyg-1(it25)* line to strain CB4856 10 successive times. Analysis of SNPs in OC118 demonstrated that all chromosomes were of Hawaiian origin except for a small region surrounding the *zyg-1* locus. To map, we crossed OC118 males with *zyg-1(it25); szy* hermaphrodites. F_1 outcross hermaphrodites were allowed to produce an F_2 generation and F_2 progeny were scored individually for the presence of the suppressor. Equal numbers of Szy-positive and Szy-negative F_2 individuals were then analyzed for a set of 18 SNP markers (three per chromosome: left arm, right arm, and center) by bulked segregant analysis (Wicks *et al.* 2001). Suppressors were further localized to a specific genetic interval on each chromosome using standard three-factor mapping techniques (Brenner 1974). As many of the morphological markers used for mapping made scoring for suppression difficult, we often tested for the presence of a recessive suppressor by backcrossing marked recombinants to the original *zyg-1(it25); szy* line and scoring unmarked F_1 for suppression.

In the course of our mapping experiments, we discovered that one of our lines carried two genetically linked suppressors: *sun-1(bs12)* and *szy-18(bs53)*. In the *zyg-1(it25)* strain, the *sun-1(bs12) szy-18(bs53)* chromosome conferred robust suppression and, in an otherwise wild-type background, a temperature-sensitive embryonic lethal phenotype. At a cytological level, this chromosome conferred two defects: loss of close association between the centrosome and the nucleus and an S-phase delay. On the basis of the genetic map position of the suppressor and the detached centrosome phenotype we decided to sequence the *sun-1* locus on this chromosome and identified a single-base substitution. As loss of *sun-1* activity does not cause an S-phase delay (Malone *et al.* 2003), we postulated the existence of a second suppressor. Fortuitously, the *sun-1(bs12)* mutation was found to disrupt an *Aci*I site and thus could be followed in crosses using snip–SNP technology. To separate the two suppressors, we isolated Sma-nonUnc and Unc-nonSma recombinants from a parental strain of genotype *zyg-1(it25)* II; *sma-1(e30)* + + *unc-76(e911)/+ sun-1(bs12) szy-18(bs53)* +. Analysis of the recombination data confirmed the existence of two suppressors and revealed that the *szy-18(bs53)* mutation segregated with relatively strong suppression and embryonic lethality marked by the S-phase delay while the *sun-1(bs12)* mutation segregated with weaker suppression, no embryonic lethality, and the detached centrosome phenotype.

Complementation tests were employed to determine if recessive and weakly semidominant mutations that mapped to a common genetic interval were allelic. In all tests, males of genotype *zyg-1(it25); szy* were mated to *zyg-1(it25); szy* hermaphrodites carrying a morphological marker that conferred a Dpy, Unc, or Egl phenotype. For each test, four unmarked F_1 progeny were picked to a 35-mm plate and incubated at 24° for 2 days. Hermaphrodites were removed and the next day the number of live progeny on the plate was counted. All appropriate *zyg-1(it25); szy* parental controls were tested in parallel. Two suppressors were scored as noncomplementing when the number of viable progeny on the test plate was equal to or greater than the number of viable progeny found on either parental control plate.

To remove the *zyg-1(it25)* mutation from the suppressor lines, we used one of the following strategies. For unlinked suppressors, we crossed males heterozygous for one of the *gfp*-marked balancer chromosomes with *zyg-1(it25); szy* hermaphrodites to create F_1 progeny of genotype *zyg-1(it25)/zyg-1(+); szy/balancer::gfp*. From these hermaphrodites, two or more *zyg-1(+); szy/balancer::gfp* lines were identified. Non-green (*szy/szy*) progeny were then isolated from each line. To separate

suppressors that mapped to the right of *dpy-10 on* chromosome II, we crossed *zyg-1(it25) szy* hermaphrodites with *dpy-10(e128) unc-4(e120)/++* males and selected *zyg-1(it25) + szy +/+ dpy-10(e128) + unc-4(e120)* F_1 progeny. These were picked individually to 35-mm plates and allowed to produce progeny. From this generation we picked Dpy-non-Unc recombinants and isolated lines homozygous for the recombinant chromosome [possible genotypes *dpy-10(e128)* or *dpy-10(e128) szy*]. As the probability of recovering a line carrying a given *szy* mutation was <100%, we isolated and analyzed at least six independent recombinant lines per suppressor. Where possible, suppressor lines were examined for the presence of a number of different phenotypes at 16°, 20°, and 25°. These phenotypes include embryonic lethality, larval lethality, and a *h*igh *i*ncidence of *m*ales (Him) phenotype, as well as anatomical defects. Lines marked with the *dpy-10(e128)* mutation could not be scored at 16° due to a partially penetrant cold-sensitive embryonic lethal phenotype associated with this morphological marker.

To test for allele specificity among the unlinked suppressors, we crossed males of genotype *zyg-1(or409) unc-4(e120)/++*; *balancer::gfp/+* with *szy* hermaphrodites. Several F_1 Gfp-positive progeny were picked to individual plates and allowed to produce progeny. From these, *zyg-1(or409) unc-4(e120)/++*; *szy/balancer::gfp* hermaphrodites were identified and several F_2 Gfp-negative Unc progeny [genotype *zyg-1(or409) unc-4(e120); szy*] were picked and used to establish a line. As a control, in parallel we reintroduced the same suppressor mutations into a *zyg-1(it25) unc-4(e120)* strain using the same strategy. To test for suppression, four L4 larvae from each strain were transferred in parallel to individual 35-mm plates and the plates were incubated at 24° for 2 days. Each plate was then scored for the presence of viable progeny.

Bypass suppression was tested by removing any residual *zyg-1* activity in each *zyg-1(it25) szy* strain using an RNAi feeding protocol (Timmons and Fire 1998). For each *zyg-1(it25) szy* line, L2 larvae were transferred to MYOB plates containing 1 mM IPTG and 25 mg/ml carbenicillin and seeded with *E. coli* HT115(DE3) pCK13. These plates were incubated at 20° until larvae reached the L4 stage at which time the plates were transferred to 24°. To assess the ability of each *szy* allele to bypass *zyg-1*, we determined the percentage of viable progeny produced during the period of maximal inactivation of *zyg-1* (48–72 hr after initial exposure to dsRNA). Controls not subjected to RNAi were processed in parallel.

Molecular biology: To create the *zyg-1(RNAi)* plasmid pCK13, we amplified a 732-bp fragment of *zyg-1* cDNA with the primers 5′-gaagatctaaaggtggattcggcgttgta-3′ and 5′-gaagatctagtgttctctcgagaagattaccgc-3′. The amplified fragment was digested with *Bgl*II and cloned into the *Bgl*II site of the RNAi feeding vector L4440 (Timmons and Fire 1998). For RNAi of *zyg-12* and *sun-1*, we used the corresponding clones from the RNAi feeding library (MRC Gene Service). Amplified genomic DNA was analyzed by automated fluorescent dye-terminator sequencing on an ABI Prism 3730xl sequencer (Seqwright).

Antibodies, immunostaining, and microscopy: DM1A, an anti-α-tubulin monoclonal antibody, was obtained from Sigma (St. Louis). The affinity-purified rabbit anti-SPD-2 polyclonal antibody was described previously (Kemp *et al.* 2004). The ZYG-1 antibody was raised in rabbits against a purified fusion protein consisting of ZYG-1 amino acids 201–402 fused to maltose-binding protein. ZYG-1-specific antibodies were affinity purified using a second fusion protein consisting of the same portion of ZYG-1 fused to glutathione *S*-transferase. This antibody detects ZYG-1 at centrioles throughout the cell cycle with highest levels at anaphase in agreement with published results (O'Connell *et al.* 2001; Dammermann *et al.* 2004; Delattre *et al.* 2006). The specificity of this antibody in immunofluorescence microscopy experiments was confirmed by staining embryos depleted of ZYG-1 by RNAi. Such embryos showed a reproducible and significant reduction in centrosome staining (data not shown). All primary antibodies were used at either 1:500 or 1:1000 dilutions. Alexa fluor 488 goat anti-rabbit and 568 goat anti-mouse secondary antibodies were from Molecular Probes (Eugene, OR). Each was used at a 1:1000 dilution. Immunostaining, spinning-disk confocal microscopy, and four-dimensional differential interference contrast (4D-DIC) microscopy were as described previously (O'Connell 2000; O'Connell *et al.* 2000; Kemp *et al.* 2004) and utilized a Plan Apo 100× 1.4-NA lens. For confocal microscopy we used a Nikon Eclipse E800 microscope equipped with a Perkin-Elmer (Norwalk, CT) Ultra*VIEW* spinning disk unit and a Hamamatsu C9100-12 EM-CCD camera. Confocal images were acquired using Openlab software and gain, offset, and gamma adjustments were made with Photoshop. For 4D-DIC microscopy, we used IPLab software to acquire images from a Zeiss Axiovert 200M microscope equipped with a Hamamatsu ORCA-ER camera.

RESULTS

Identification of *zyg-1* suppressors: In the *C. elegans* embryo, loss of *zyg-1* gene activity results in a failure of centrosome duplication (O'Connell *et al.* 2001). As a consequence, bipolar spindles are not assembled, DNA is not properly segregated, cytokinesis fails, and the embryos die. ZYG-1 is distantly related to vertebrate PLK4, a kinase that is also required for centriole replication (Bettencourt-Dias *et al.* 2005; Habedanck *et al.* 2005). As key regulators of duplication, the activity of these kinases is likely stringently controlled. To identify factors that interact with *zyg-1* to regulate centrosome duplication we designed a sensitive genetic suppressor screen to identify mutations that restore normal centrosome duplication to an embryo deficient in *zyg-1* activity (Figure 1A). Animals homozygous for the temperature-sensitive partial loss-of-function allele *zyg-1(it25)* appear wild type at 16° but exhibit a fully penetrant embryonic lethal phenotype at 25° (Kemphues *et al.* 1988a). The mutant form of the protein encoded by *zyg-1(it25)* contains a single-amino-acid substitution (P442L) in the nonkinase portion of ZYG-1 (Figure 3A), but still localizes to centrosomes (Figure 4A). To identify suppressors, we used EMS to induce germ-line mutations in a population of *zyg-1(it25)* animals, grew this population for two generations at permissive temperature to allow any suppressor mutations to become homozygous, and then shifted the population to the restrictive temperature to select for those suppressor-bearing individuals. There were three key features of our experimental design. First, to make screening as efficient as possible, we sought to minimize the number of animals screened without reducing the complexity of the pool. We reasoned that since each F_1 mother produces many progeny carrying the same EMS-induced mutation, we needed to assay only a small fraction of progeny. Thus, we treated the F_1 population with hypochlorite to kill all animals except for the small clutch of F_2 eggs present

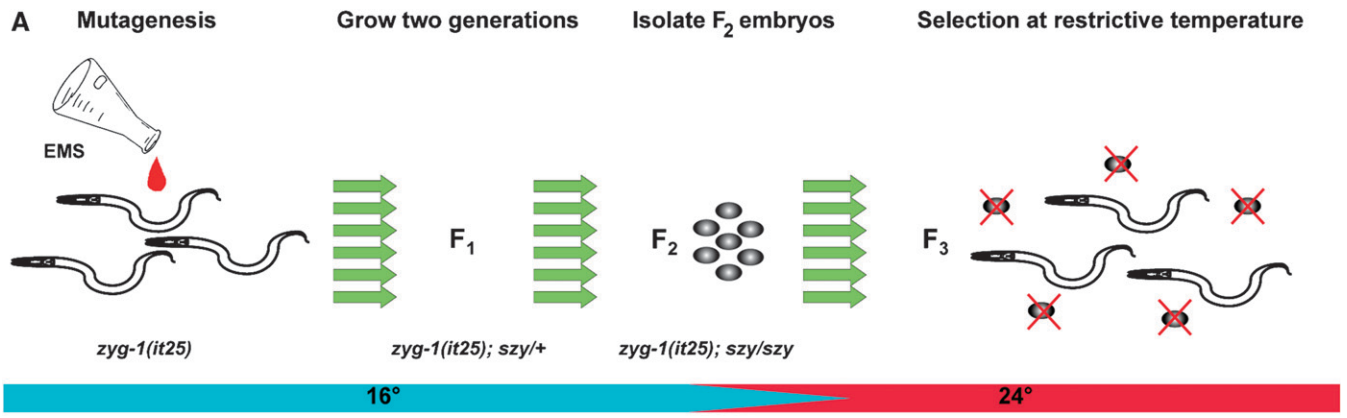

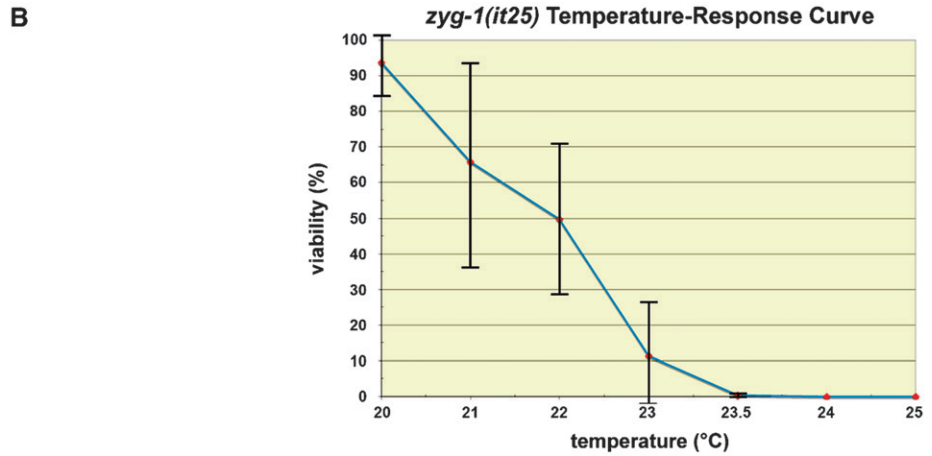

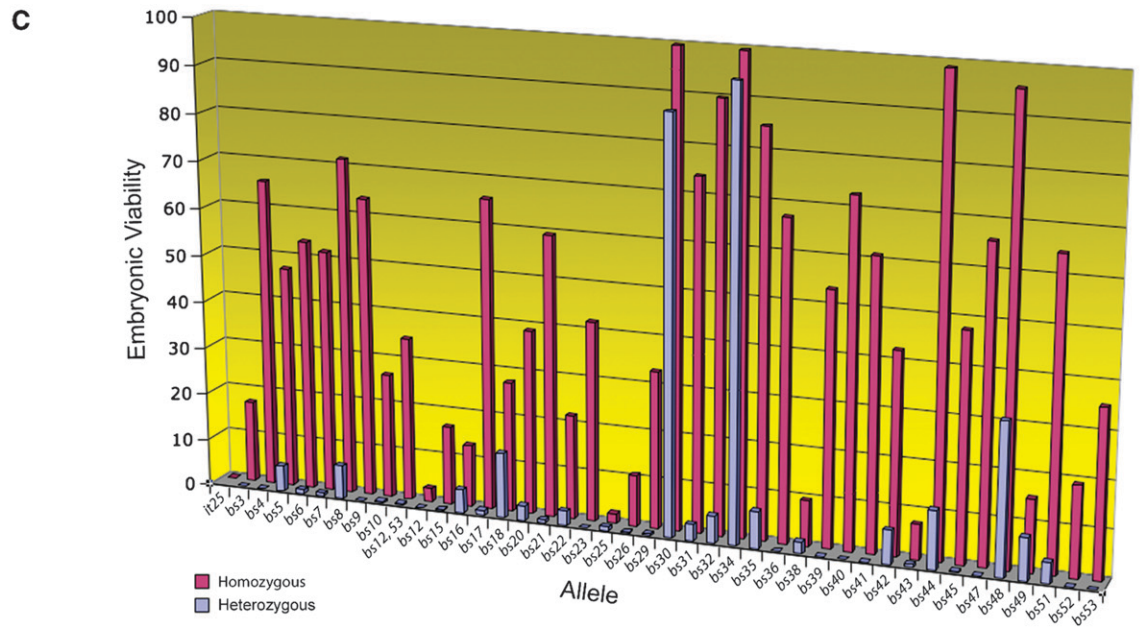

FIGURE 1.—Suppressor screen. (A) To identify mutations that restore centrosome duplication and viability to a strain compromised for *zyg-1* function, animals carrying the temperature-sensitive mutation *zyg-1(it25)* were treated with EMS. At the permissive temperature, EMS-induced germ-line *szy* mutations are transmitted to the F_1 generation in the heterozygous state (*szy*/+) and to the F_2 generation in the homozygous state (*szy*/*szy*). To identify *szy*-bearing individuals, F_2 embryos were isolated, allowed to complete larval development at permissive temperature, and then shifted to restrictive temperature for 3–6 weeks. *szy*-bearing lines give rise to multiple generations over this time period while all other individuals die off. The columns of green arrows indicate that individual pools of mutagenized lines were processed in parallel. To ensure independence, only one suppressor was retained from each pool. (B) Percentage of embryonic viability of a *zyg-1(it25)* strain as a function of temperature. Each data point represents the average

(Continued)

in each uterus. Second, to make our method as sensitive as possible we screened at the lowest possible temperature at which 100% of *zyg-1(it25)* embryos die. This temperature was found to be 24° (Figure 1B). At this temperature, the mutants still possess residual *zyg-1* activity but this level falls just short of that necessary to sustain viability. Third, we selected for suppressors over an extended period of time (the equivalent of 6–12 life cycles). We reasoned that this should reduce the number of false positives as suppressor-bearing lines would be required to survive over multiple generations. This feature would also allow us a greater chance of identifying suppressors with a growth defect, due either to weak suppression or to a deleterious effect caused by the suppressor mutation itself.

In a screen of an estimated 314,000 haploid genomes, we isolated 39 independent mutant lines that could reproducibly grow at 24° despite carrying the *zyg-1(it25)* mutation. One of these lines contained two genetically linked suppressor mutations that we ultimately separated and characterized independently (see MATERIALS AND METHODS). Thus we identified a total of 40 independent suppressors. After backcrossing, each of the suppressor-bearing *zyg-1(it25)* lines was assayed for the ability to grow at restrictive temperature. We found that these mutations differed markedly in their potency of suppression (Figure 1C and Table 1). A few backcrossed lines exhibited weak suppression and were assayed at 23.5° (noted in Table 1), but most of the mutant lines exhibited robust levels of viability (>20%) at 24°, including four (*bs30*, *bs34*, *bs44*, and *bs48*) that exhibited wild-type levels of viability. None of the isolated lines, however, contained a reversion of the *zyg-1(it25)* mutation; when challenged to grow at 25° all of the lines exhibited significant levels of embryonic lethality (our unpublished data). In fact, we were surprised to find that for most suppressors just a 1° increase in temperature (from 24° to 25°) resulted in a significant reduction in suppression. For instance, in the case of *zyg-1(it25)* animals carrying the *bs7* suppressor, ~50% of the offspring survived at 24° while none survived at 25°. We conclude that the restrictive temperature employed in the screen is a key determinant of stringency and can profoundly affect the results.

Genetic properties of *zyg-1* suppressors: To determine which of our suppressors are dominant and which are recessive, we determined the percentage of viable *zyg-1(it25)* embryos produced by strains heterozygous for each suppressor. Twenty-one of the 40 suppressors were found to be recessive, although about half of these heterozygotes do allow an occasional embryo to survive. However, in all cases this amounts to <2.0% of the level seen in the corresponding homozygote and thus we deemed this level of suppression insignificant. Of the remaining 19 suppressors, 15 were found to be semidominant; as heterozygotes, these mutations afforded levels of suppression that range between 4.7 and 38.2% of the corresponding homozygous levels. Just four of the suppressors—*bs18*, *bs30*, *bs34*, and *bs49*—were found to be truly dominant. When heterozygous, these mutations are ≥50% as effective as when homozygous. Thus, the design of our screen allowed the identification of a genetically diverse set of suppressors.

Suppressors can work through a variety of mechanisms. Bypass suppressors work by rewiring the process under study so that the gene being suppressed is no longer needed. Other suppressors work by restoring activity to the suppressed gene or, conversely, by lowering the requirement for that gene. With respect to the present study, bypass suppressors would work in a manner that would render centrosome duplication (and suppression) completely independent of *zyg-1*. For example, some suppressors might activate a centrosome-independent spindle assembly pathway as described in vertebrates (KHODJAKOV *et al.* 2000). Alternatively, nonbypass suppressors would work to restore the normal process of duplication utilizing the residual *zyg-1* activity present in the *zyg-1(it25)* mutant. To determine by which mechanism each of our suppressors work, we used RNAi to remove the residual *zyg-1* activity present in each suppressor strain and then assayed for suppression. Strikingly, none of these strains were able to grow when residual *zyg-1* activity was eliminated (Table 1). Thus, none of the suppressors identified in this screen bypass *zyg-1*. The most likely explanation for this result is that the ZYG-1-dependent centrosome duplication pathway is indispensable for proper embryonic cell division. These results also indicate that all *szy* suppressors work by increasing the residual activity of the *zyg-1(it25)* allele or conversely by reducing the level of *zyg-1* needed for successful centrosome duplication.

***zyg-1* activity is regulated by a large number of *szy* genes:** To determine how many genes were represented by this set of suppressor mutations and to position these genes for further study, we determined the genetic map position of each of the 40 mutations. We found that the suppressor mutations are distributed on four of six *C. elegans* chromosomes (Figure 2). Interestingly, we mapped 26 suppressors to chromosome II within the vicinity of *zyg-1*, initially leading us to believe that most of the mutations that we had identified were intragenic suppressors. However, this was not the case. Additional

percentage of viability among the offspring of four to five individuals shifted as L4 larvae to the indicated temperature for 24 hr. The vertical bars indicate the standard deviation. Note that the largest standard deviations are observed at the intermediate temperatures of 21°–23°. (C) Potency of *szy* alleles. Each *szy* allele in the homozygous (red) or heterozygous (blue) state was assayed for suppression of *zyg-1(it25)* embryonic lethality. Shown is the average percentage of viable offspring. Numerical values including standard deviations and the number of embryos scored are listed in Table 1 along with assay conditions and complete strain genotypes.

TABLE 1

Genetics of suppression

Strain	Temperature	*szy/szy*			*szy/+*		
		Average[a]	SD	*N*[b]	Average[a]	SD	*N*[b]
Potency of *szy* alleles in homozygous and heterozygous state							
zyg-1(it25)	23.5°	0	0	194			
zyg-1(it25)	24°	0	0	1852			
zyg-1(bs8 it25)	24°	71.5	6.9	240	7.2	7	458
zyg-1(bs18 it25)	24°	27.6	9	342	13.8	13.8	321
zyg-1(bs30 it25)	24°	99.7	0.7	253	87.5	6.6	282
zyg-1(bs34 it25)	24°	99.6	0.8	224	94.6	2.6	286
zyg-1(bs44 it25)	24°	98.8	1.8	298	12.4	8.2	267
zyg-1(bs48 it25)	24°	95.8	2.7	272	32	9	208
zyg-1(it25); sun-1(bs12)[c]	24°	2.8[d]	2.7	1307	0[d]	0	1501
zyg-1(it25); sun-1(bs12) szy-18(bs53)	24°	34.6	12.5	277	0.4	1.3	415
szy-1(bs3); zyg-1(it25)	24°	17.2	19.7	150	0	0	207
zyg-1(it25); szy-2(bs4)	24°	65.5	11.8	283	0	0	427
zyg-1(it25) szy-3(bs5)	24°	47.1	21.1	216	5.5	5.9	301
zyg-1(it25) szy-4(bs6)	24°	53.3	22.1	261	0.9	1	270
zyg-1(it25) szy-4(bs17)	24°	65.7	6.9	214	1.1	2.1	266
zyg-1(it25) szy-4(bs23)	24°	42.2	31.8	210	0	0	211
szy-5(bs7); zyg-1(it25)	24°	51.5	18.9	193	0.7	1.4	284
zyg-1(it25) szy-6(bs9)	24°	63.5	10.7	311	0	0	263
zyg-1(it25) szy-7(bs10)	24°	26.4	17.7	271	0.4	1.2	573
zyg-1(it25) szy-7(bs41)	24°	61.1	11.2	251	0	0	310
zyg-1(it25); szy-8(bs15)	24°	16.6	10.4	176	0.21	0.66	503
zyg-1(it25) szy-9(bs20)	24°	38.9	14.5	343	3.1	1.2	288
zyg-1(it25) szy-9(bs25)	24°	2.1	1.5	290	0.8	1	243
zyg-1(it25) szy-9(bs26)	24°	10.8	4.3	332	0.2	0.6	949
zyg-1(it25) szy-9(bs32)	24°	89.9	10.1	165	5.8	9	337
zyg-1(it25) szy-9(bs40)	24°	72.8	10	405	0	0	299
zyg-1(it25) szy-9(bs45)	24°	47.9	14.4	265	0.3	0.6	350
zyg-1(it25) szy-10(bs21)	24°	59.4	11.3	207	0.7	0.8	295
zyg-1(it25); szy-11(bs22)	24°	22	24.2	494	3.1	5.2	591
zyg-1(it25); szy-12(bs16)	23.5°	13.1	6	376	5	3	543
szy-13(bs29) zyg-1(it25)	24°	33.1	15.4	239	0.4	0.8	285
zyg-1(it25) szy-14(bs31)	24°	74	12.7	279	3.5	5.4	528
zyg-1(it25) szy-14(bs38)	24°	9.7	10.9	404	2.5	2	264
szy-15(bs35); zyg-1(it25)	23.5°	85	13.2	187	7.8	9.3	350
zyg-1(it25) szy-16(bs36)	24°	67.3	16.9	242	0	0	278
zyg-1(it25); szy-17(bs39)	24°	53.5	25.5	177	0	0	303
zyg-1(it25); szy-17(bs42)	24°	42.5	21	340	7.2	4.3	181
zyg-1(it25); szy-17(bs43)	24°	7.4	7.8	266	0.7	0.9	676
zyg-1(it25); szy-17(bs47)	24°	66	27	390	0	0	308
zyg-1(it25); szy-17(bs51)	23.5°	64.8	17.4	414	4.5	2.7	520
zyg-1(it25); szy-18(bs53)[e]	24°	35.3	5.6	295	0	0	584
zyg-1(it25) szy-19(bs49)	24°	15.3	7.1	368	9	2	269
zyg-1(it25) szy-20(bs52)	24°	19.2[d]	14.5	552	0[d]	0	484

(*continued*)

mapping placed 16 of these suppressors to the right of *dpy-10* and therefore outside of the interval containing the *zyg-1* locus. As most of our suppressor mutations do not map near loci known to be required for centrosome replication (*spd-2*, *sas-4*, etc.), these mutations appear to define genes not previously implicated in this process.

Through genetic mapping and genomic sequencing, we determined that 6 of the 40 suppressors are intragenic suppressors. Each of these mutations—*bs8*, *bs18*, *bs30*, *bs34*, *bs44*, and *bs48*—were mapped to within <1 map unit of the *zyg-1* locus and all were found to exhibit some degree of dominance as expected for intragenic mutations. We sequenced the entire *zyg-1* locus in each of these mutants and in every case identified a unique single-base-pair substitution (Figure 3A). The mutation *bs30* results in a G-to-A transition 3 bp upstream of the initiator methionine codon, suggesting that it affects expression of *zyg-1*. The mutations *bs8*,

TABLE 1

(Continued)

Strain	Temperature	Suppression on control plates			Suppression on RNAi plates		
		Average[a]	SD	N^b	Average[a]	SD	N^b
Test for *zyg-1* bypass suppression of *szy* alleles							
zyg-1(it25)	24°	0.04	0.2	4258	0	0	4038
zyg-1(it25); sun-1(bs12) szy-18(bs53)	24°	45.7	5.9	583	0	0	438
szy-1(bs3); zyg-1(it25)	24°	32.5	20.5	276	0	0	301
zyg-1(it25); szy-2(bs4)	24°	71.3	28.7	606	0	0	536
zyg-1(it25) szy-3(bs5)	24°	6.0	4.2	456	0	0	565
zyg-1(it25) szy-4(bs6)	24°	93.8	4.7	339	0	0	540
zyg-1(it25) szy-4(bs17)	23.5°	98.5	2.0	381	0	0	193
zyg-1(it25) szy-4(bs23)	24°	46.6	29.1	3950	0	0	132
szy-5(bs7); zyg-1(it25)	24°	16.9	11.5	238	0	0	504
zyg-1(it25) szy-6(bs9)	24°	42.7	7.1	548	0	0	554
zyg-1(it25) szy-7(bs10)	24°	60.0	11.0	358	0	0	307
zyg-1(it25) szy-7(bs41)	24°	26.0	18.1	363	0	0	439
zyg-1(it25); szy-8(bs15)	24°	36.2	13.1	198	0	0	197
zyg-1(it25) szy-9(bs20)	24°	17.2	9.5	429	0	0	482
zyg-1(it25) szy-9(bs25)	24°	32.4	21.8	330	0	0	445
zyg-1(it25) szy-9(bs26)	24°	9.6	8.6	355	0	0	522
zyg-1(it25) szy-9(bs32)	24°	38.6	8.5	273	0	0	343
zyg-1(it25) szy-9(bs40)	24°	21.6	6.2	236	0	0	412
zyg-1(it25) szy-9(bs45)	24°	29.7	7.9	384	0	0	612
zyg-1(it25) szy-10(bs21)	24°	4.9	6.7	483	0	0	218
zyg-1(it25); szy-11(bs22)	23.5°	86.8	7.6	301	0	0	436
zyg-1(it25); szy-12(bs16)	24°	31.3	9.8	222	0	0	403
szy-13(bs29) zyg-1(it25)	24°	49.3	21.6	374	0	0	501
zyg-1(it25) szy-14(bs31)	24°	37.3	16.1	449	0.5	0.9	412
zyg-1(it25) szy-14(bs38)	24°	23.0	25.1	907	0	0	472
szy-15(bs35); zyg-1(it25)	24°	44.8	22.2	353	0	0	481
zyg-1(it25) szy-16(bs36)	24°	24.1	1.6	414	0	0	297
zyg-1(it25); szy-17(bs39)	24°	24.1	12.4	268	0	0	187
zyg-1(it25); szy-17(bs42)	24°	14.5	10.4	401	0	0	308
zyg-1(it25); szy-17(bs43)	23.5°	11.4	9.9	568	0.4	0.8	497
zyg-1(it25); szy-17(bs47)	24°	22.8	1.8	472	0	0	404
zyg-1(it25); szy-17(bs51)	24°	18.2	5.2	413	0	0	484
zyg-1(it25) szy-19(bs49)	24°	13.2	8.0	455	0	0	588
zyg-1(it25) szy-20(bs52)	24°	57.9	44.9	282	0	0	265

[a] Average percentage of embryonic viability.

[b] Number of embryos tallied.

[c] The complete genotype of the strain tested was *zyg-1(it25); sun-1(bs12) szy-18(bs53) +/sun-1(bs12) + unc-76(e911)*. The congenic strain *zyg-1(it25); sun-1(bs12) szy-18(bs53) unc- 76(e911)/+ + +* served as a negative control and produced 0 ± 0 viable progeny ($n = 1501$).

[d] Measurement made 24–48 hr after shift to restrictive temperature. All other values reported in the top were measured during the first 24 hr after the shift to restrictive temperature.

[e] The complete genotype of the strain tested was *zyg-1(it25); sma-1(e30) + szy-18(bs53)/+ sun-1(bs12) szy-18(bs53)*. The strain *zyg-1(it25); sun-1(bs12) szy-18(bs53) unc-76(e911)/+ + +* served as a negative control and produced 0 ± 0 viable progeny ($n = 1501$).

bs18, *bs34*, *bs44*, and *bs48* each result in a predicted single-amino-acid substitution within the C-terminal half of *zyg-1* where all previously studied mutations, including *it25* and *or409*, are known to reside. Interestingly, only one of these suppressors, *bs44*, affects an amino acid residue conserved between *C. elegans* and the related species *C. briggsae* (Figure 3B). This is in stark contrast to the four loss-of-function mutations all of which affect conserved residues. This result is not unexpected given that conserved residues are likely critical for function and that most mutagenic changes in this group of residues would render the protein nonfunctional. The positions of suppressor mutations, however, appear to be less constrained, with both conserved and nonconserved residues affected.

To obtain an estimate of the number of genes defined by the 34 extragenic suppressors, we performed complementation tests on all closely linked recessive and semidominant mutations (see MATERIALS AND METHODS). Because the *bs49* mutation is dominant, we were unable to subject it to complementation analysis with closely linked suppressor mutations. As this mutation is unique

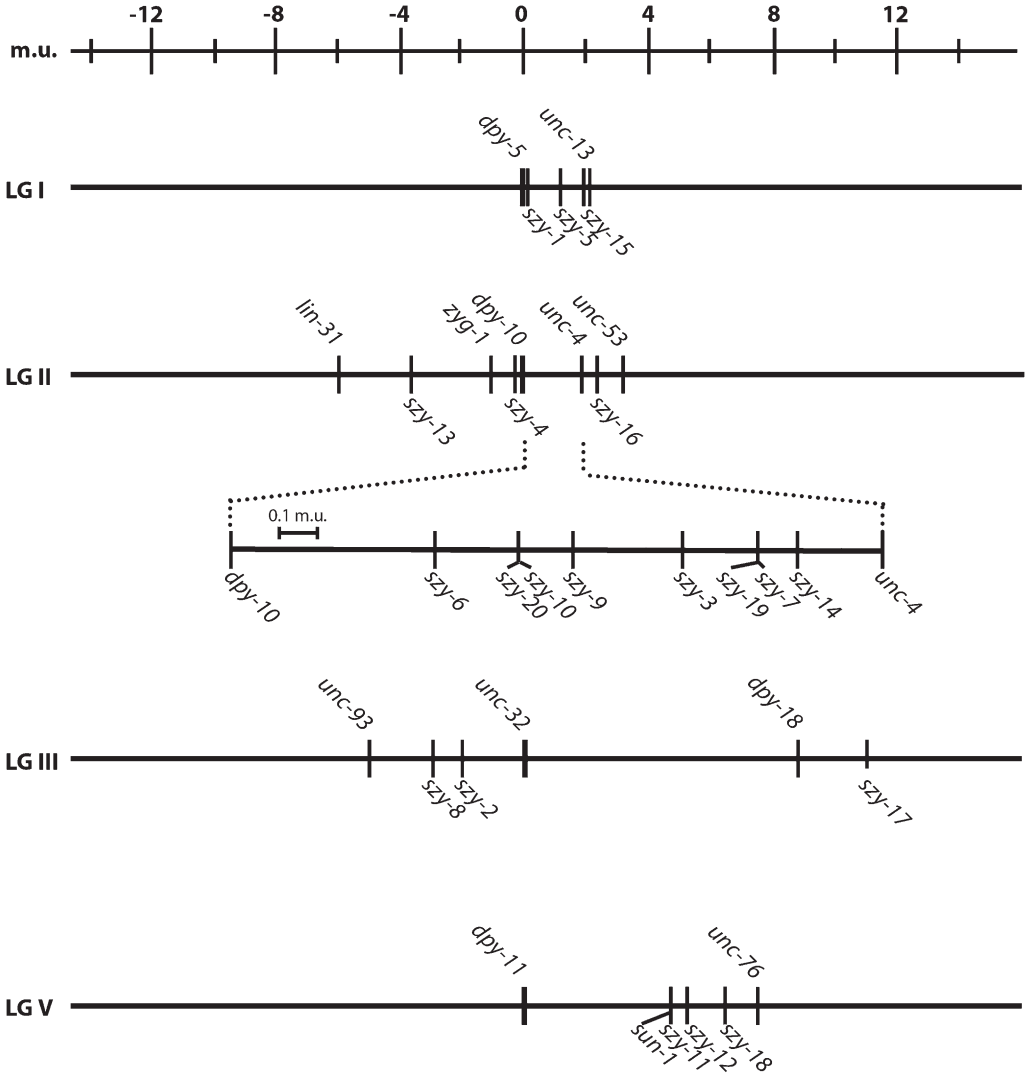

FIGURE 2.—Genetic map showing location of *szy* genes. Note that the relative ordering of some *szy* genes within the *dpy-10-unc-4* interval is not known with certainty.

in that it was the only fully dominant extragenic suppressor identified, we assigned it as an allele of a distinct gene. Interestingly, we found that our set of *zyg-1* suppressor mutations defines a surprisingly large number of genes. In total, our data indicate that this set of mutations comprises 21 distinct genes, which we refer to as *szy* (***s**uppressor of **zy**g-1*) genes. However, as described below, the *bs12* mutation was found to be an allele of the *sun-1* gene and thus we utilize the established nomenclature. Sixteen of these genes are defined by a single allele. Of the remaining 5 *szy* genes, 2 are defined by two alleles, 1 by three alleles, 1 by five alleles, and 1 by six alleles. Given that so many of the *szy* genes are defined by one allele, we believe the screen is not yet saturated and that additional genes can be mutated to produce a suppressor phenotype.

Having established map positions, we next addressed whether our collection contained allele-specific suppressors. Allele-specific suppressors suppress only one mutant allele of the target gene and are more likely to define genes whose products physically interact with the targeted gene's product. Due to the tight linkage between *zyg-1* and 11 of the *szy* genes, we were unable to test allele specificity in these cases—we were able to separate most of the linked suppressors from the original *zyg-1* mutation but we were not able to design an effective strategy to reintroduce a *zyg-1* mutation. We did, however, test at least one allele of each of the 10 unlinked *szy* genes. Suppressor mutations, once separated from the original *zyg-1(it25)* mutation, were crossed back into a *zyg-1(it25)* background, as well as into a *zyg-1(or409)* background. The *zyg-1(or409)* allele confers a temperature-sensitive phenotype similar in severity to that of the *zyg-1(it25)* allele (our unpublished data), yet, at the molecular level, *zyg-1(or409)* is distinct from *zyg-1(it25)*, resulting in a ZYG-1 protein with an amino acid substitution that differs from *zyg-1(it25)* (Figure 3). Although we did not quantify the level of suppression in this test, all suppressor mutations tested—*szy-1(bs3)*, *szy2-(bs4)*, *szy-5(bs7)*, *sun-1(bs12)*, *szy-8(bs15)*, *szy-12(bs16)*, *szy-11(bs22)*, *szy-15(bs35)*, *szy-(bs39)*, and *szy-18(bs53)*—allowed both the *zyg-1(it25)* and *zyg-1(or409)*

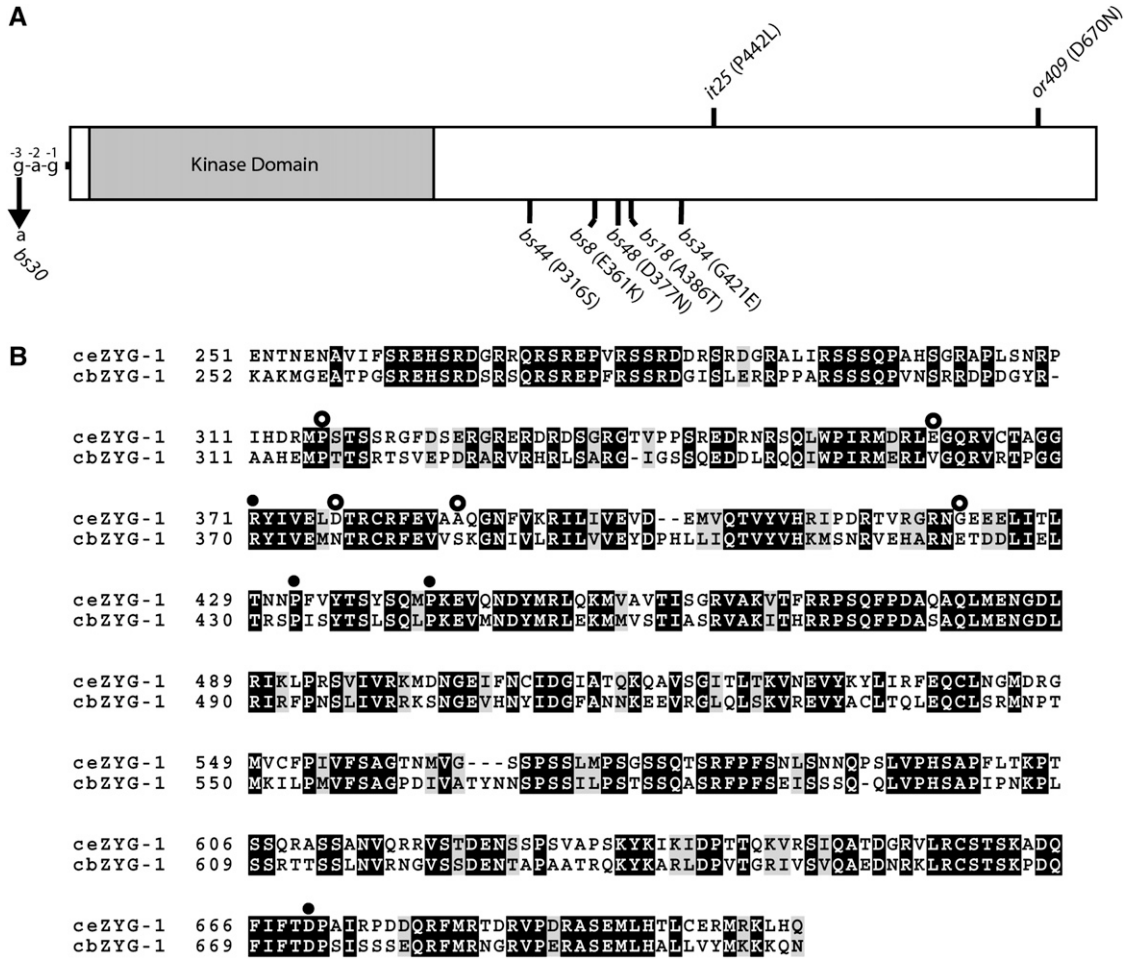

FIGURE 3.—Intragenic *zyg-1* suppressors. (A) Schematic of the ZYG-1 protein showing the positions of the *zyg-1(it25)* and *zyg-1(or409)* mutations and the six intragenic suppressors. Five suppressor mutations are within the coding region and the presumptive amino acid substitutions are indicated. The *bs30* mutation is a G-to-A transition 3 bp upstream of the initiator methionine codon. (B) Amino acid sequence alignment of the nonkinase portions of ZYG-1 from *C. elegans* and *C. briggsae*. Identical and similar amino acid residues are shown as solid and shaded areas, respectively. Solid circles indicate the positions of the four known loss-of-function mutations. Open circles indicate the positions of the five suppressor mutations that produce an amino acid substitution.

mutants to grow at the restrictive temperature. Thus, alleles of all 10 genes tested do not exhibit allele specificity, suggesting that the majority of mutations identified in this screen are capable of suppressing more than one allele of *zyg-1*.

***szy* mutations suppress the centrosome duplication defect of *zyg-1(it25)* mutants:** We next investigated possible mechanisms whereby the extragenic suppressors restored viability to *zyg-1* mutants. One obvious possibility is that the normal process of centrosome duplication is restored. However, it is also possible that other mechanisms are at work. For instance, some *szy* mutations might allow centrioles to form *de novo* rather than through the normal templated pathway (MARSHALL *et al.* 2001). As mentioned above, some suppressors could also function by activating a centrosome-independent spindle assembly mechanism. To address these issues, we analyzed spindle assembly in wild-type, *zyg-1(it25)*, and *zyg-1(it25); szy* double-mutant embryos. Using immunofluorescence microscopy, we examined microtubule organization and ZYG-1 distribution at all stages between first anaphase and second telophase. In wild-type embryos, ZYG-1 can be detected as a single dot at the poles of the first mitotic spindle until late anaphase when the two centrioles of a pair separate giving rise to two dots (Figure 4A). At each spindle pole, one of the dots represents a sperm-derived centriole while the other dot marks a centriole synthesized during the initial round of centrosome duplication following fertilization. During the second cell cycle of wild-type embryos, ZYG-1 can be detected at the center of each centrosome/spindle pole as either one dot representing a centriole pair prior to anaphase or later two dots representing the separated centrioles (Figure 4B).

In *zyg-1(it25)* mutants, we found that ZYG-1 could still localize to centrioles ($n = 41$ embryos). At most cell

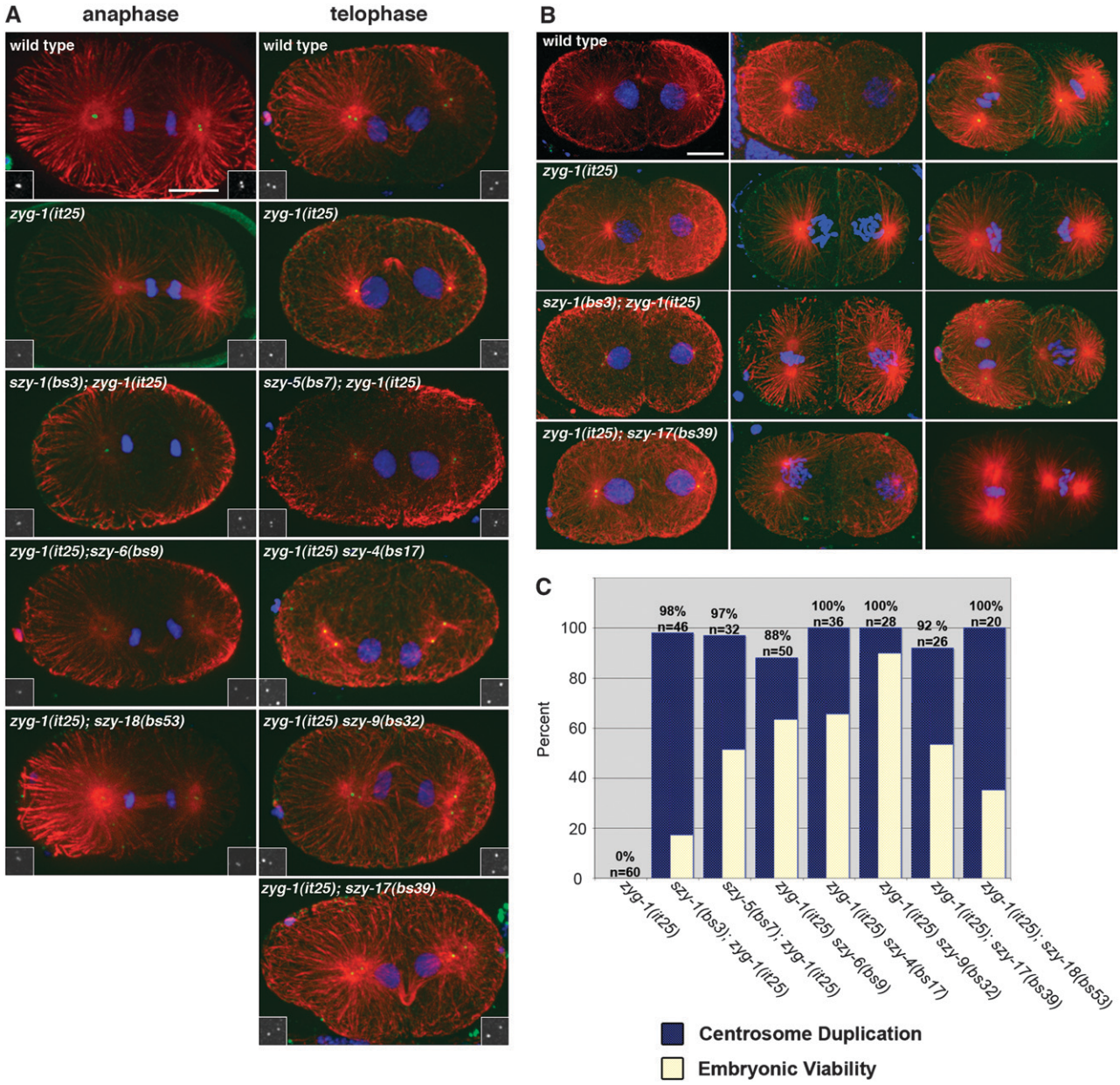

FIGURE 4.—Centrosome duplication is restored in *zyg-1(it25)*; *szy* mutants. (A and B) Images of wild-type, *zyg-1(it25)*, and *zyg-1(it25)*; *szy* double mutants stained for tubulin (red), DNA (blue), and ZYG-1 (green). (A) Embryos are in anaphase (left column) or telophase (right column). Insets show ZYG-1 staining at spindle poles. Note that at telophase *zyg-1(it25)* embryos have only a single dot of ZYG-1 at each pole while all other strains clearly have two, indicating successful centrosome duplication. Bar, 10 μm. (B) Microtubule-organizing activity is similar during the second cell cycle in the wild-type and *zyg-1(it25)*; *szy* double mutants. Shown are images of wild-type, *zyg-1(it25)*, and *zyg-1(it25)*; *szy* embryos at early (left column), mid (center column), and late (right column) points of the second cell cycle. In wild-type and *zyg-1(it25)*; *szy* double mutants microtubule-organizing centers appear similar in size, number, and position, indicating that the normal process of centrosome duplication has been restored. Bar, 10 μm. (C) Quantification of centrosome duplication in *zyg-1(it25)* and *zyg-1(it25)*; *szy* double mutants. Centrosome duplication was assessed for each strain by scoring two-cell stage blastomeres in late prophase for the presence of two centrosomes. Blue columns indicate the percentage of successful duplication events. The actual value is shown above the column with the number of duplication events scored. For comparison, the level of embryonic viability of each strain is shown in yellow.

cycle stages, we found that there were no discernable differences between wild-type and *zyg-1(it25)* mutants in the centriole levels of ZYG-1. In anaphase, however, most wild-type embryos appeared to possess more centriole-associated ZYG-1 than did the *zyg-1(it25)* mutants (Figure 4A). This difference appeared transient as the wild type and the mutant invariably possessed similar centriole levels at telophase. *zyg-1(it25)* embryos also never contained more than a single dot of ZYG-1 at each pole of the first mitotic spindle, indicative of a failure to duplicate the sperm-derived centrioles. In two-cell stage *zyg-1(it25)* embryos, we continued to detect a

TABLE 2

Phenotypes of *szy* alleles

Strain	Temperature	Plate phenotype[a]				Cytological defects
		Defect	% Emb[b]	SD[c]	N[d]	
sun-1(bs12)[e]	25°	None	1.2	1.1	772	Detached centrosomes
szy-1(bs3)	20°	Emb, Him, Lva	45.1	12.4	1099	Detached centrosomes, elongated centrosomes
szy-2(bs4)	25°	Emb ts	61.8	14.9	632	Anaphase bridging of chromatin
szy-5(bs7)	25°	Emb ts, Him	74.1	14.7	174	Complex phenotype: abnormal microtubule cytoskeleton, supernumerary centrosomes and chromosomes, detached centrosomes
szy-8(bs15)	20°	Emb ts	10.8	10.8	512	Detached centrosomes
szy-10(bs21)[f]	25°	Emb ts	81.3	11.7	104	Supernumerary centrosomes and chromosomes
szy-11(bs22)	25°	Him	ND[g]	ND	ND	ND
szy-14(bs31)[f]	25°	Slow growth	ND	ND	ND	ND
szy-14(bs38)[f]	25°	Slow growth	ND	ND	ND	ND
szy-15(bs35)	25°	Emb ts	54.9	14.2	280	Consistent defect not detected
szy-18(bs53)[h]	25°	Emb ts	93.8	7.9	536	Abnormal cell cycle timing
szy-17(bs51)	25°	Him	ND	ND	ND	ND
szy-20(bs52)[f]	25°	Emb ts, Him	54.3	ND	186	Complex phenotype: abnormal microtubule cytoskeleton, abnormal cell cycle, detached centrosomes, defective cytokinesis

[a] Phenotypes scored on plates with a dissecting microscope include embryonic lethality (Emb), high incidence of males (Him), larval arrest (Lva), and slow growth. Temperature-sensitive (ts) designation indicates the phenotype was significantly more severe or more fully penetrant at 25°.
[b] Average percentage of embryos that fail to hatch.
[c] Standard deviation.
[d] Number of embryos tested.
[e] Complete strain genotype: *zyg-1(it25)/+; sun-1(bs12) + unc-76(e911)/sun-1(bs12) szy-18(bs53) +*.
[f] All contained the *dpy-10(e128)* marker.
[g] Not done.
[h] Complete strain genotype: *zyg-1(it25)/+; sma-1(e30) + szy-18(bs53)/+ sun-1(bs12) szy-18(bs53)*.

single dot of ZYG-1 at the center of each centrosome, but we never observed more than one microtubule-organizing center per blastomere (Figure 4B).

We next analyzed spindle assembly and ZYG-1 distribution in embryos from seven *zyg-1(it25)*; *szy* double-mutant lines: *szy-1(bs3)*; *zyg-1(it25)* ($n = 28$), *szy-5(bs7)*; *zyg-1(it25)* ($n = 26$), *zyg-1(it25) szy-6(bs9)* ($n = 22$), *zyg-1(it25) szy-4(bs17)* ($n = 30$), *zyg-1(it25) szy-9(bs32)* ($n = 19$), *zyg-1(it25)*; *szy-17(bs39)* ($n = 19$), and *zyg-1(it25)*; *szy-18(bs53)* ($n = 28$). For all seven strains, we observed that the first bipolar spindle often contained poles with two ZYG-1 dots (Figure 4A), indicating that the first round of centrosome duplication had been executed properly. As in the wild type, the two ZYG-1 dots first became apparent during late anaphase. At the two-cell stage, bipolar spindles were assembled at a high frequency in all seven lines (Figure 4C). As in the wild type, ZYG-1 staining indicated that all spindles in the double mutants contained centrioles at the poles (Figure 4B and our unpublished observations). We did not observe any evidence of acentriolar spindle formation, nor did we observe any indication that centrioles were arising *de novo*. The number and position of ZYG-1 positive dots in the *zyg-1(it25)*; *szy* double mutants were similar to those in wild type during the first (Figure 4A) and second (Figure 4B) cell cycles, suggesting that the normal pathway of centriole replication was being executed. However, in the absence of ultrastructural analysis, we cannot rule out the possibility of *de novo* centriole formation.

To determine if any of the *szy* mutations affect the localization of ZYG-1, we compared ZYG-1 staining in the double-mutant lines with that in the wild-type and the *zyg-1(it25)* line. We found that at all stages examined, all of the *zyg-1(it25)*; *szy* double mutants possessed centrosome-associated levels of ZYG-1 that were similar to that of the parental *zyg-1(it25)* line. Thus, for this set of szy mutants, we do not find evidence that suppression occurs as a result of an increase in the centrosome-associated levels of ZYG-1.

***szy* genes function in a variety of cellular processes:** Some suppressor mutations confer phenotypes of their own. This is particularly true in cases where the mutation is in an essential gene. To determine if any of our suppressor mutations confer phenotypes on their own, we constructed *zyg-1(+)* derivatives of 30 of the 34 extragenic suppressors—the *szy-4* and *szy-13* alleles were too tightly linked to *zyg-1* to remove the *zyg-1(it25)* mutation. For each suppressor, multiple independent *zyg-1(+)* derivatives were analyzed for growth defects at 25°, 20°, and where possible 16°. Interestingly, 12 of the 30 suppressors exhibit an observable phenotype (Table 2). Eight of the suppressors—*szy-1(bs3)*, *szy-2(bs4)*,

szy-5(bs7), *szy-8(bs15)*, *szy-10(bs21)*, *szy-15(bs35)*, *szy-20(bs52)*, and *szy-18(bs53)*—were found to exhibit an embryonic lethal phenotype. In addition, the *szy-1(bs3)* mutant exhibits a partially penetrant larval arrest phenotype and a Him phenotype. Likewise the *szy-5(bs7)*, *szy-11(bs22)*, *szy-17(bs51)*, and *szy-20(bs52)* mutants each possess a Him phenotype. The Him phenotype arises due to meiotic chromosome segregation defects that result in loss of the sex (X) chromosome and the production of X/O male progeny. Finally, we found that both alleles of the *szy-14* gene—*bs31* and *bs38*—confer a slow growth phenotype that appears to be due to smaller than normal brood sizes. Surprisingly, the phenotypes exhibited by most of these mutants are temperature sensitive; for *szy-2(bs4)*, *szy-5(bs7)*, *szy-8(bs15)*, *szy-15(bs35)*, *szy-20(bs52)*, and *szy-18(bs53)*, significantly higher levels of embryonic lethality were observed at 25° than at lower temperature. Likewise, the Him phenotypes of *szy-11(bs22)* and *szy-17(bs51)* were observed only at 25° and the slow growth phenotypes of the *szy-14* alleles were found to be most severe at 25°. Conditional alleles are relatively rare and thus it was surprising to identify so many temperature-sensitive mutations.

It is possible that *zyg-1(it25)* and one or more of the *szy* mutations exhibit mutual suppression. That is, not only would a *szy* mutation suppress *zyg-1(it25)* defects, but also the *zyg-1(it25)* mutation would suppress *szy* defects. A comparison of the numbers reported in Tables 1 and 2 would seem to suggest that animals carrying *szy-5(bs7)*, *szy-10(bs21)*, *szy-15(bs35)*, or *szy-18(bs53)* all grow better if the *zyg-1(it25)* mutation is also present. However, one should be careful to note that these *zyg-1(it25)*; *szy* double mutants were assayed for growth at 23.5° and 24° (Table 1), while the corresponding *szy* single mutants were assayed at 25° (Table 2). To assess the ability of the *zyg-1(it25)* mutation to suppress a *szy* mutation the single and double mutants need to be assayed at the same temperature. Indeed when the *szy-5(bs7)* mutant is assayed at 24°, rather than at 25°, we find that the level of embryonic lethality drops to 31.4 ± 18.2% ($n = 262$). Thus at this temperature, 68.6% of *szy-5(bs7)* embryos survive. In comparison, only 51.5% of *szy-5(bs7)*; *zyg-1(it25)* embryos survive at 24° (Table 1). Therefore at 24° we find no evidence of mutual suppression. Nonetheless, it is still possible that *zyg-1(it25)* suppresses one or more of the *szy* mutations including *szy-5(bs7)*, but such a determination will require growth comparisons over a range of temperatures.

The embryonic lethal phenotypes associated with some of the *szy* mutations suggest that the corresponding genes are important for normal embryonic development. To determine what roles these genes play, we cytologically examined lines carrying the embryonic lethal mutations by immunostaining gonads and embryos for tubulin, DNA, and centrosomes. Most of these suppressor mutants were found to exhibit clearly observable phenotypes. The most striking phenotype is that associated with the *szy-5(bs7)* mutant. In 52% of these embryos ($n = 27$), tubulin staining revealed the presence of large cytoplasmic structures. In some of the most severely affected *szy-5(bs7)* embryos, the robust arrays of microtubules observed in wild-type embryos are completely absent, with all tubulin appearing in an aggregated form (Figure 5B). These aggregates were also found throughout the hermaphrodite germ line (Figure 5C). We also observed that 56% ($n = 27$) of *szy-5(bs7)* embryos possess cells with an excess of centrosomes and DNA. It is likely that in many cases this phenotype is due to cytokinesis failure as a consequence of the tubulin aggregation defect. However, we found several examples of *szy-5(bs7)* embryos carrying extra centrosomes and DNA that lacked the tubulin aggregates (Figure 5D). This suggests that *szy-5(bs7)* mutants possess two independent defects: tubulin aggregation and supernumerary centrosomes/chromosomes. The origin of the extra centrosomes in these *szy-5(bs7)* embryos is not currently clear. Given that all embryos with an excess number of centrosomes also contained an excess number of chromosomes, the most plausible explanation is a defect in cytokinesis. Live imaging of *szy-5(bs7)* embryos will be needed to address this issue.

A variety of severe defects were observed in *szy-20(bs52)* embryos. Multinucleate cells with supernumerary centrosomes were observed in 32% ($n = 22$) of *szy-20(bs52)* embryos (Figure 5E). Live-imaging analysis revealed that this defect arises from cytokinesis failure (our unpublished observations). *szy-20(bs52)* embryos also display defects in other processes (Table 2). A tubulin aggregation phenotype similar to but less severe than that of *szy-5(bs7)* embryos was observed in 10% ($n = 40$) of *szy-20(bs52)* embryos (Figure 5F). Interestingly, in both *szy-5(bs7)* and *szy-20(bs52)* animals, centriole proteins, such as SPD-2 (Figure 5F) and ZYG-1 (our unpublished observations), also appear in aggregate form. In some instances these aggregates colocalize with the tubulin aggregates but in other instances they do not. There are a number of possible explanations for this phenotype. For example, centriole proteins might be aggregating in response to an inappropriately activated centrosome replication pathway or centrosomes might be undergoing fragmentation. Additional molecular, cytological, and genetic analysis should be helpful in distinguishing between the various possibilities.

Like the *szy-5(bs7)* and *szy-20(bs52)* mutants, embryos carrying the *szy-10(bs21)* mutation were found to possess multinucleate cells with supernumerary centrosomes (17%, $n = 12$ embryos) (Figure 5G). These embryos, however, lack the protein aggregation phenotype seen in the *szy-5(bs7)* and *szy-20(bs52)* mutants. As is the case with *szy-5(bs7)* and *szy-20(bs52)*mutants, the excess centrosomes of *szy-10(bs21)* embryos are always accompanied by an excess of chromosomes, suggesting a defect in cytokinesis.

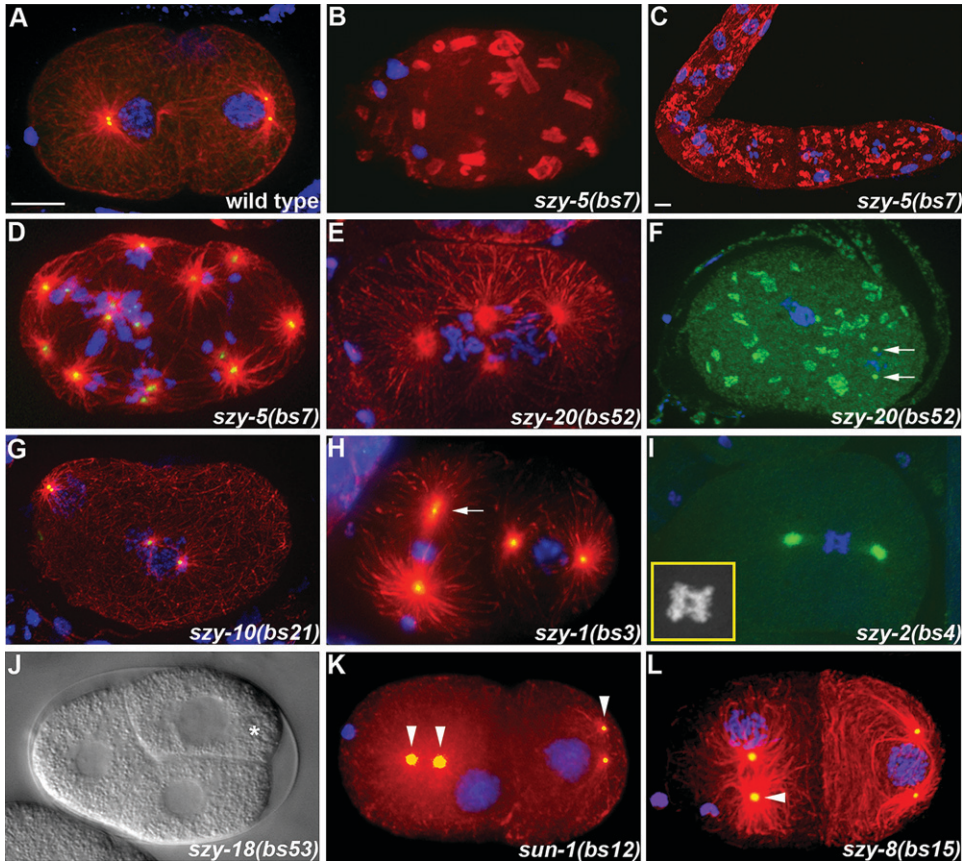

FIGURE 5.—*szy* genes are required for proper cell division. Confocal (A–I, K, and L) or DIC (J) images of *szy* mutants are shown. Confocal images are maximal-intensity projections of multiple optical sections of embryos/gonads stained for tubulin (red) and/or DNA (blue). Some embryos are also stained for centrosomes (green) with antibodies to SPD-2 (A, D, F–I, K, and L). (A) A wild-type embryo at the beginning of the two-cell stage. (B) A *szy-5(bs7)* one-cell embryo and (C) proximal gonad showing the tubulin aggregation phenotype. (D) A one-cell *szy-5(bs7)* embryo and (E) a one-cell *szy-20(bs52)* embryo each with excess centrosomes and DNA. (F) A one-cell *szy-20(bs52)* embryo with cytoplasmic aggregates of SPD-2. Arrows indicate centrosomes. (G) A multinucleated *szy-10(bs21)* embryo with multiple centrosomes. (H) A two-cell *szy-1(bs3)* embryo with an elongated centrosome (arrow). (I) A *szy-2(bs4)* embryo with anaphase bridging of chromatin. Inset shows a magnified view of chromatin. (J) A *szy-18(bs53)* embryo with an unusual three-cell configuration resulting from delayed division of the P_1 blastomere (asterisk). (K) Two-cell *sun-1(bs12)* and (L) *szy-8(bs15)* embryos displaying detached centrosomes (arrowheads). Bars in A and C, 10 μm.

The *szy-1(bs3)*, *szy-2(bs4)*, and *szy-18(bs53)* mutants each possess a defect that is unique among the *szy* mutants. In 66% ($n = 32$) of *szy-1(bs3)* embryos, some centrosomes were found to exhibit an odd morphological defect. Affected centrosomes have an elongated appearance (Figure 5H). Many spindles were observed that possessed one elongated pole and one normal-looking pole although some spindles with two elongated poles were observed. The *szy-2(bs4)* mutation affects the separation of chromosomes. In 50% of the mutant embryos ($n = 14$), we observed blastomeres containing chromatin bridges between the separating sets of anaphase chromosomes (Figure 5I). There is an interesting developmental aspect to this phenotype, as the later divisions seem to be affected more than the earlier divisions. In contrast, the *szy-18(bs53)* mutation affects cell cycle timing. Wild-type embryos exhibit asynchronous divisions beginning at the two-cell stage where the anterior blastomere AB divides ~2 min ahead of its posterior sister P_1 (BRAUCHLE *et al.* 2003). We noted that in *szy-18(bs53)* embryos this asynchrony is exaggerated with P_1 dividing on average 10.5 min ($n = 6$ embryos) after AB. This timing defect results in embryos with an unusual three-cell configuration (Figure 5J). Interestingly, this phenotype has been noted to occur when DNA synthesis is inhibited (ENCALADA *et al.* 2000; BRAUCHLE *et al.* 2003). In such cases, AB and P_1 are delayed in S phase, but P_1 is delayed to a much greater extent than AB. Similarly, we found that the underlying cause of this phenotype is an S-phase delay (our unpublished data). Further analysis will be needed to determine if the *szy-18(bs53)* mutation identifies a pathway regulating S phase and its associated events such as DNA synthesis and centriole duplication.

Interestingly, six of the suppressor mutations confer a common phenotype: loss of close association between the centrosome and nuclear envelope. This "detached centrosome" defect was observed in 54% ($n = 28$) of *sun-1(bs12)* embryos (Figure 5K), in 64% ($n = 11$) of *szy-8(bs15)* embryos (Figure 5L), and in 23% ($n = 22$) of *szy-5(bs7)* embryos (our unpublished observations). Embryos carrying the *szy-1(bs3)*, *szy-10(bs21)*, or *szy-20(bs52)* mutations also occasionally exhibit this defect. In *sun-1(bs12)* mutant embryos, centrosome detachment was most often observed during the early part of the cell cycle when the microtubule asters organized by the centrosomes were relatively small. This detachment appears to be only temporary as prophase-stage blastomeres typically were found to possess centrosomes and nuclei in close association. Despite this defect, there is no significant embryonic lethality associated with the *sun-1(bs12)* mutation (Table 2), indicating that continuous

association between the nucleus and the centrosome is not essential for viability.

The *sun-1* gene is a regulator of centrosome duplication: As a mechanistic link between centrosome duplication and nuclear association had not been previously established, the identification of genes that participate in linking the centrosome to the nucleus was an unexpected outcome of our screen. To begin to understand the mechanisms that tie centrosome–nuclear attachment to duplication, we set out to molecularly identify one of the suppressors with a detached centrosome phenotype and discovered that the *bs12* mutation is an allele of the *sun-1* gene. We accomplished this by mapping the *bs12* mutation to the right arm of chromosome V between the morphological markers *sma-1* and *unc-76*. Within this 3.18-Mbp region of DNA, the only gene known to have a role in attaching the centrosome to the nucleus is *sun-1* (Malone *et al.* 2003). We therefore sequenced the *sun-1* genomic region in the *bs12* mutant and found a single G-to-A transition in a conserved residue within the 5′-splice site of the third intron. Translation of the improperly spliced message would be expected to produce a truncated protein lacking a putative transmembrane domain and the conserved C-terminal SUN domain. As noted, *sun-1(bs12)* is a weak allele with no effect on embryonic viability (Table 2), and thus this mutation likely reduces, but does not eliminate, proper splicing of the *sun-1* message.

Our results indicate that SUN-1 is a negative regulator of ZYG-1. Yet, the *sun-1(bs12)* mutation only marginally affects the viability of the *zyg-1(it25)* mutant (Figure 1C and Table 1). Given that *sun-1(bs12)* is a weak allele, the lack of a robust effect might be due to insufficient inactivation of *sun-1*. To address this, we used RNAi to silence expression of *sun-1* in the *zyg-1(it25)* strain and assayed suppression. Under these conditions we still observed only weak suppression of the embryonic lethal phenotype (3.5%, $n = 367$). However, under the same conditions, RNAi of *sun-1* in wild-type worms resulted in a high level (87%, $n = 209$) of embryonic lethality. Given that almost 90% of the embryos die due to loss of *sun-1* activity, the highest level of suppression one could expect to observe would be ~10%. Thus, the high level of lethality caused by RNAi of *sun-1* precluded us from utilizing embryonic viability as an accurate readout for suppression.

We therefore chose to assay the effect of *sun-1(RNAi)* directly on centrosome duplication using two approaches. One approach was to stain fixed embryos for tubulin, DNA, and ZYG-1. We analyzed 31 one- and two-cell *zyg-1(it25)* embryos that had been subjected to *sun-1(RNAi)*. Silencing of *sun-1* severely impaired the association of centrosomes and nuclei and led to chromosome segregation defects and aneuploidy. Unfortunately, this made it extremely difficult to accurately assign developmental stages to affected embryos. Nevertheless we found numerous two-cell *zyg-1(it25)*; sun-1(RNAi) embryos with evidence of centrosome duplication (Figure 6A). In most instances, we could clearly detect ZYG-1 staining at the center of these centrosomes, indicating that centrioles were present and that suppression by *sun-1(RNAi)* involved restoration of centriole replication. In these experiments we also compared the level of ZYG-1 staining between the 31 *zyg-1(it25)*; *sun-1(RNAi)* embryos and 26 *zyg-1(it25)* embryos that were mock-RNAi treated (*i.e.*, those that were grown on bacteria carrying only the empty RNAi feeding vector L4440). If suppression is due to an increase in ZYG-1 levels at the centrosome, we might expect that centrioles in *zyg-1(it25)*; *sun-1(RNAi)* embryos would stain more intensely than controls. However, we found that *zyg-1(it25)* embryos subject to *sun-1(RNAi)* did not

A

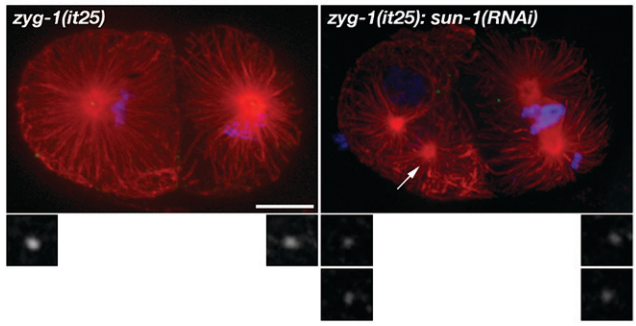

B

Strain	First Cell Cycle		Second Cell Cycle		Third Cell Cycle		Percent Rescue
	·)	·—·)	·)	·—·)	·)	·—·)	
zyg-1(it25)	0	20	40	0	22	0	0
zyg-1(it25); sun-1(RNAi)	0	8	15	1	10	6	22
zyg-12 (RNAi) zyg-1(it25)	1	17	35	0	16	0	0

Figure 6.—*sun-1(RNAi)*, but not *zyg-12(RNAi)*, suppresses the centrosome duplication defect in *zyg-1(it25)* mutants. (A) *zyg-1(it25)* and *zyg-1(it25)*; *sun-1(RNAi)* embryos were stained for microtubules (red), DNA (blue), and ZYG-1 (green). The *zyg-1(it25)*; *sun-1(RNAi)* embryo exhibits evidence of centrosome duplication as well as loss of contact between a nucleus and a centrosome (arrow). Insets show threefold magnified views of ZYG-1 staining at centrosomes. Bar, 10 μm. (B) Spindle assembly in *zyg-1* embryos depleted of SUN-1 or ZYG-12. Embryos were isolated from mothers grown at 24° and early development was analyzed by 4D-DIC imaging at the same temperature. In columns 2–7, the number of spindle assembly events resulting in either a monopolar (·) or a bipolar (·—·) spindle is tallied for the first three cell cycles. Note that not all embryos were scored for the third cell cycle. In the last column, the percentage of bipolar spindles formed, indicating successful centrosome duplication, is shown.

appear to possess any more centrosome-associated ZYG-1 than controls. In fact, some embryos subject to *sun-1(RNAi)* appeared to have less ZYG-1 present at centrioles than control embryos (Figure 6A). Thus, we do not find evidence that loss of SUN-1 activity results in elevated levels of ZYG-1 at the centrosome.

We used a second approach to more accurately measure the ability *of sun-1(RNAi)* to suppress the centrosome duplication defect of *zyg-1(it25)* mutants. Specifically, we used 4D-DIC imaging to follow bipolar spindle formation during the first several cell cycles in *zyg-1(it25)* and *zyg-1(it25); sun-1(RNAi)* embryos. In this assay, assembly of a bipolar spindle indicates a successful centriole duplication event during the previous cell cycle, while assembly of a monopolar spindle indicates failure. At 24°, control *zyg-1(it25)* embryos exhibit a complete block to centriole duplication (Figure 6B). In such embryos, the first spindle is always bipolar ($n = 20$ events) owing to the separation of the sperm-donated centrioles. However, these centrioles invariably fail to duplicate, resulting in the formation of monopolar spindles in all blastomeres during the second and third cell cycles ($n = 62$ events). In *zyg-1(it25); sun-1(RNAi)* embryos the first spindle is also invariably bipolar. However, depletion of *sun-1* allowed 7 of 32 blastomeres to assemble a bipolar spindle during the second and third cell cycles. Curiously, the effect of depleting *sun-1* on centrosome duplication is more apparent during the third cell cycle than during the second cell cycle (Figure 6B). This could indicate a more significant role for SUN-1 in these later cell cycles or else that less *zyg-1* activity is needed later in development. In any event, this result confirms that suppression arises as a result of loss of *sun-1* activity, indicating that SUN-1 antagonizes the activity of ZYG-1.

SUN-1 has distinct roles in centrosome duplication and nuclear association: Our identification of SUN-1 at once suggests the presence of a novel regulatory mechanism governing centrosome duplication. We envision two alternative models. It is possible that SUN-1 in concert with at least some other components of the centrosome–nucleus attachment complex operates in a direct manner to regulate centrosome duplication. In such a scenario, these proteins would be bifunctional, operating to anchor the centrosome to the nucleus and independently to regulate duplication. Alternatively, these proteins might function in an indirect manner to regulate centrosome duplication simply through their ability to maintain association between the centrosome and nucleus. The nucleus might be associated with an inhibitor of duplication, and thus by tethering the centrosome to the nucleus SUN-1 might maintain contact between the centrosome and this inhibitory signal.

The indirect model predicts that any condition that detaches the centrosome from the nucleus will suppress *zyg-1* mutations. To test this model we sought to break the nucleus–centrosome connection via other means. In addition to SUN-1, the hook-related protein ZYG-12 is known to be required for proper centrosome–nucleus attachment (Malone *et al.* 2003). Interestingly, we did not identify alleles of *zyg-12* in our screen. This might be due to the lack of saturation in our screen or alternatively that inhibition of *zyg-12* does not suppress *zyg-1* loss-of-function mutations. To investigate a potential role for ZYG-12 in centrosome duplication, we performed *zyg-12(RNAi)* in a *zyg-1(it25)* background and assayed for suppression. Since *zyg-12* is an essential gene, we decided to assay the effect of *zyg-12(RNAi)* on centrosome duplication directly by analyzing spindle assembly in 4D-DIC recordings of *zyg-1(it25)* embryos depleted of *zyg-12* by RNAi. In most of the *zyg-12(RNAi) zyg-1(it25)* embryos examined ($n = 18$) we observed a dramatic loss of association between the centrosomes and the nucleus, indicating that we had significantly inhibited *zyg-12* activity (our unpublished data). However, all 51 spindle-assembly events recorded during the second and third cell cycles resulted in formation of monopolar spindles (Figure 6B). Thus, despite significant inhibition of *zyg-12*, the *zyg-1(it25)* centrosome duplication phenotype is not suppressed. This result demonstrates that suppression does not simply result from freeing centrosomes from the nuclear envelope, indicating that *sun-1* functions to regulate centrosome duplication independent of its role in centrosome–nuclear attachment.

DISCUSSION

The isolation and characterization of suppressors provide a powerful approach to uncover the mechanisms regulating centrosome replication. Historically, the application of suppressor genetics led to one of the most important discoveries in the centrosome field. γ-Tubulin, a central player in microtubule nucleation, was first identified in the fungus Aspergillus in a screen for mutations that suppress the lethality of a temperature-sensitive β-tubulin mutation (Weil *et al.* 1986; Oakley and Oakley 1989). In applying this approach to a *zyg-1* mutant, we have identified 21 genes with potentially important roles in regulating centrosome duplication and thus have laid the foundation for future studies aimed at understanding regulatory inputs that provide temporal and spatial control of this process.

A number of the suppressor mutations identified in our screen appear to define essential genes as they are associated with lethal phenotypes. This demonstrates that the design of our screen successfully cleared a major hurdle, as essential genes can be particularly difficult to identify via this approach. On the one hand, strong loss-of-function mutations in essential genes might strongly suppress the *zyg-1* duplication defect but cause such a debilitating growth defect of their own

that they would be missed. On the other hand, weaker alleles might not cause a significant growth defect but also might not be potent enough to suppress *zyg-1* lethality. On the basis of the results, our screen appears sensitive enough to identify both strong and weak alleles of essential genes (Figure 1C and Table 2). For instance, we identified the mutation *szy-1(bs3)*, which while producing a significant level of embryonic lethality of its own still modestly suppresses *zyg-1* lethality, and we identified a very weak allele of the essential gene *sun-1*.

An important issue with suppressor screens is specificity: How many of the suppressors identify genes that have a functionally relevant interaction with the target gene? For instance, collagen mutations have been found to suppress temperature-sensitive *glp-1* mutations in *C. elegans* (Maine and Kimble 1989), and indeed in the course of our work we found that some collagen mutations also provide modest suppression of *zyg-1* (our unpublished data). However, on the basis of map position and phenotypic analysis it appears that our screen filtered out this nonspecific class of suppressors. A second line of evidence supporting the specificity of our approach is our cytological analysis, which has demonstrated that many of the *szy* mutants have centrosome or microtubule-related defects (Figure 5). Third, we have cloned one of these *szy* genes (*sun-1*) and found it to be a gene with an established centrosome-related function (Malone *et al.* 2003). These three lines of evidence argue that many of the genes identified here are specifically involved in the process of centrosome duplication.

Given these arguments for the specificity of our approach, why are there so many *szy* genes? In fact, on the basis of the large fraction of *szy* genes defined by a single allele (16 of 21), this screen is not yet saturated and thus more *szy* genes must exist. One possible explanation for this surprising result might be that there are multiple inputs that regulate *zyg-1* activity. For instance, *zyg-1* activity might be regulated as a means to coordinate duplication with other cell cycle events, to ensure that centrosomes are not replicated more than once per cell cycle or to prevent the *de novo* formation of centrioles (Delattre and Gonczy 2004). Thus the large number of *szy* genes might simply reflect the presence of multiple regulatory circuits that fine tune *zyg-1* activity. Alternatively, or in addition, *zyg-1* activity might be governed by a large multisubunit complex and loss of activity of any one constituent could compromise *zyg-1* regulation.

In light of the fact that many of our *szy* mutants share at least one phenotype in common—detached centrosomes—it is tempting to speculate that the factors encoded by these genes assemble into a multifunctional complex that anchors the centrosome to the nuclear envelope while also regulating duplication. One of these factors is SUN-1, a member of a conserved family of inner nuclear envelope proteins that play pivotal roles in linking the nucleus to the microtubule or actin cytoskeletons (Starr and Fischer 2005). SUN-domain-containing proteins target adapter proteins such as ZYG-12 (Malone *et al.* 2003) or the actin-binding protein ANC-1 (Starr and Han 2002) to the outer nuclear envelope. We found, however, that SUN-1-dependent regulation of centrosome duplication does not involve ZYG-12. These results show that the role played by SUN-1 in centrosome duplication is distinct from its role in providing a physical linkage between the centrosome and the nucleus. Recently, Mps3, a homolog of SUN-1, has been shown to be required for duplication of the yeast spindle pole body, an organelle analogous to the animal centrosome (Jaspersen *et al.* 2006). Our finding differs, as we define a negative role for SUN-1 in centrosome duplication rather than the positive role described in this recent work. This might indicate that SUN-domain-containing proteins play a complex role in this process or else that the function of such proteins has changed over the course of evolution. Further analysis should help clarify this issue.

Nuclear proteins are emerging as important regulators of the centrosome and microtubule cytoskeleton. Spindle assembly factors such as TPX2 and NuMA are sequestered in the nucleus during interphase (Harel and Forbes 2004), and the nucleolar protein nucleophosmin associates with centrosomes and inhibits their duplication (Okuda *et al.* 2000). These factors are all under the control of the small GTPase Ran, a key regulator of nucleocytoplasmic transport (Harel and Forbes 2004; Wang *et al.* 2005). RanGTP functions in this capacity by antagonizing the activity of importins that bind to and inhibit TPX2 and NuMA. Also, RanGTP in a complex with the export receptor Crm1 promotes association of nucleophosmin with centrosomes. Intriguingly, disruption of the Ran/importin regulatory cascade in *C. elegans* results in some phenotypes that are similar, though not identical, to those observed in our screen (Askjaer *et al.* 2002). These include detached centrosomes, chromatin bridges, and P_1 cell cycle delays. However, the map position of most *szy* genes does not coincide with that of Ran or its known effectors and thus if Ran is involved in ZYG-1 regulation, some *szy* genes might represent a new class of Ran effectors.

The identification of *szy* genes has provided us the opportunity to begin to address the mechanisms that regulate centrosome duplication. Further study of the *szy* genes, including molecular analysis, should allow us to quickly dissect the regulatory networks involved. In some cases we are likely to establish new ties to existing cellular processes as suggested by the phenotypic similarity of some our mutants to the defects that arise when other vital processes are perturbed. Equally as important, some of our mutants have novel phenotypes, such as the striking protein aggregation phenotype seen in *szy-5* and *szy-20* mutants, suggesting completely novel forms of regulation. Thus, analysis of the *szy* genes is likely to provide important insights into centrosome

duplication and to once again validate the power of genetics in tying together seemingly unrelated cellular processes.

We thank Kevin Kopish for technical assistance; Edward Kipreos for helpful suggestions; and Andy Golden, Kathryn Stein, and Nick Miliaras for comments on the manuscript. This research was supported by the Intramural Research Program of the National Institutes of Health (NIH) and by the National Institute of Diabetes and Digestive and Kidney Diseases. Some nematode strains used in this work were provided by the *Caenorhabditis* Genetics Center, which is funded by the NIH National Center for Research Resources.

LITERATURE CITED

Askjaer, P., V. Galy, E. Hannak and I. W. Mattaj, 2002 Ran GTPase cycle and importins alpha and beta are essential for spindle formation and nuclear envelope assembly in living *Caenorhabditis elegans* embryos. Mol. Biol. Cell **13:** 4355–4370.

Azimzadeh, J., and M. Bornens, 2004 The centrosome in evolution, pp. 93–122 in *Centrosomes in Development and Disease*, edited by E. A. Nigg. Wiley-VCH GmbH, Weinheim, Germany.

Bettencourt-Dias, M., A. Rodrigues-Martins, L. Carpenter, M. Riparbelli, L. Lehmann *et al.*, 2005 SAK/PLK4 is required for centriole duplication and flagella development. Curr. Biol. **15:** 2199–2207.

Bobinnec, Y., A. Khodjakov, L. M. Mir, C. L. Rieder, B. Edde *et al.*, 1998 Centriole disassembly in vivo and its effect on centrosome structure and function in vertebrate cells. J. Cell Biol. **143:** 1575–1589.

Brauchle, M., K. Baumer and P. Gonczy, 2003 Differential activation of the DNA replication checkpoint contributes to asynchrony of cell division in *C. elegans* embryos. Curr. Biol. **13:** 819–827.

Brenner, S., 1974 The genetics of *Caenorhabditis elegans*. Genetics **77:** 71–94.

Cassada, R., E. Isnenghi, M. Culotti and G. von Ehrenstein, 1981 Genetic analysis of temperature-sensitive embryogenesis mutants in *Caenorhabditis elegans*. Dev. Biol. **84:** 193–205.

Church, D. L., K. L. Guan and E. J. Lambie, 1995 Three genes of the MAP kinase cascade, *mek-2, mpk-1/sur-1* and *let-60* ras, are required for meiotic cell cycle progression in *Caenorhabditis elegans*. Development **121:** 2525–2535.

Dammermann, A., T. Muller-Reichert, L. Pelletier, B. Habermann, A. Desai *et al.*, 2004 Centriole assembly requires both centriolar and pericentriolar material proteins. Dev. Cell **7:** 815–829.

Delattre, M., and P. Gonczy, 2004 The arithmetic of centrosome biogenesis. J. Cell Sci. **117:** 1619–1630.

Delattre, M., S. Leidel, K. Wani, K. Baumer, J. Bamat *et al.*, 2004 Centriolar SAS-5 is required for centrosome duplication in *C. elegans*. Nat. Cell Biol. **6:** 656–664.

Delattre, M., C. Canard and P. Gonczy, 2006 Sequential protein recruitment in *C. elegans* centriole formation. Curr. Biol. **16:** 1844–1849.

Doxsey, S., 2001 Re-evaluating centrosome function. Nat. Rev. Mol. Cell. Biol. **2:** 688–698.

Encalada, S. E., P. R. Martin, J. B. Phillips, R. Lyczak, D. R. Hamill *et al.*, 2000 DNA replication defects delay cell division and disrupt cell polarity in early *Caenorhabditis elegans* embryos. Dev. Biol. **228:** 225–238.

Gonczy, P., S. Pichler, M. Kirkham and A. A. Hyman, 1999a Cytoplasmic dynein is required for distinct aspects of MTOC positioning, including centrosome separation, in the one cell stage *Caenorhabditis elegans* embryo. J. Cell Biol. **147:** 135–150.

Gonczy, P., H. Schnabel, T. Kaletta, A. D. Amores, T. Hyman *et al.*, 1999b Dissection of cell division processes in the one cell stage *Caenorhabditis elegans* embryo by mutational analysis. J. Cell Biol. **144:** 927–946.

Habedanck, R., Y. D. Stierhof, C. J. Wilkinson and E. A. Nigg, 2005 The Polo kinase Plk4 functions in centriole duplication. Nat. Cell Biol. **7:** 1140–1146.

Hamill, D. R., A. F. Severson, J. C. Carter and B. Bowerman, 2002 Centrosome maturation and mitotic spindle assembly in *C. elegans* require SPD-5, a protein with multiple coiled-coil domains. Dev. Cell **3:** 673–684.

Harel, A., and D. J. Forbes, 2004 Importin beta: conducting a much larger cellular symphony. Mol. Cell **16:** 319–330.

Hirsh, D., and R. Vanderslice, 1976 Temperature-sensitive developmental mutants of *Caenorhabditis elegans*. Dev. Biol. **49:** 220–235.

Jaspersen, S. L., A. E. Martin, G. Glazko, T. H. Giddings Jr., G. Morgan *et al.*, 2006 The Sad1-UNC-84 homology domain in Mps3 interacts with Mps2 to connect the spindle pole body with the nuclear envelope. J. Cell Biol. **174:** 665–675.

Kamath, R. S., A. G. Fraser, Y. Dong, G. Poulin, R. Durbin *et al.*, 2003 Systematic functional analysis of the *Caenorhabditis elegans* genome using RNAi. Nature **421:** 231–237.

Kemp, C. A., K. R. Kopish, P. Zipperlen, J. Ahringer and K. F. O'Connell, 2004 Centrosome maturation and duplication in *C. elegans* require the coiled-coil protein SPD-2. Dev. Cell **6:** 511–523.

Kemphues, K. J., M. Kusch and N. Wolf, 1988a Maternal-effect lethal mutations on linkage group II of *Caenorhabditis elegans*. Genetics **120:** 977–986.

Kemphues, K. J., J. R. Priess, D. G. Morton and N. S. Cheng, 1988b Identification of genes required for cytoplasmic localization in early *C. elegans* embryos. Cell **52:** 311–320.

Khodjakov, A., R. W. Cole, B. R. Oakley and C. L. Rieder, 2000 Centrosome-independent mitotic spindle formation in vertebrates. Curr. Biol. **10:** 59–67.

Kirkham, M., T. Muller-Reichert, K. Oegema, S. Grill and A. A. Hyman, 2003 SAS-4 is a *C. elegans* centriolar protein that controls centrosome size. Cell **112:** 575–587.

Leidel, S., and P. Gonczy, 2003 SAS-4 is essential for centrosome duplication in *C elegans* and is recruited to daughter centrioles once per cell cycle. Dev. Cell **4:** 431–439.

Leidel, S., M. Delattre, L. Cerutti, K. Baumer and P. Gonczy, 2005 SAS-6 defines a protein family required for centrosome duplication in *C. elegans* and in human cells. Nat. Cell Biol. **7:** 115–125.

Maine, E. M., and J. Kimble, 1989 Identification of genes that interact with *glp-1*, a gene required for inductive cell interactions in *Caenorhabditis elegans*. Development **106:** 133–143.

Malone, C. J., L. Misner, N. Le Bot, M. C. Tsai, J. M. Campbell *et al.*, 2003 The *C. elegans* hook protein, ZYG-12, mediates the essential attachment between the centrosome and nucleus. Cell **115:** 825–836.

Marshall, W. F., Y. Vucica and J. L. Rosenbaum, 2001 Kinetics and regulation of de novo centriole assembly. Implications for the mechanism of centriole duplication. Curr. Biol. **11:** 308–317.

Miwa, J., E. Schierenberg, S. Miwa and G. von Ehrenstein, 1980 Genetics and mode of expression of temperature-sensitive mutations arresting embryonic development in *Caenorhabditis elegans*. Dev. Biol. **76:** 160–174.

Oakley, C. E., and B. R. Oakley, 1989 Identification of gamma-tubulin, a new member of the tubulin superfamily encoded by *mipA* gene of *Aspergillus nidulans*. Nature **338:** 662–664.

O'Connell, K. F., 2000 The centrosome of the early *C. elegans* embryo: inheritance, assembly, replication, and developmental roles. Curr. Top. Dev. Biol. **49:** 365–384.

O'Connell, K. F., C. M. Leys and J. G. White, 1998 A genetic screen for temperature-sensitive cell-division mutants of *Caenorhabditis elegans*. Genetics **149:** 1303–1321.

O'Connell, K. F., K. N. Maxwell and J. G. White, 2000 The *spd-2* gene is required for polarization of the anteroposterior axis and formation of the sperm asters in the *Caenorhabditis elegans* zygote. Dev. Biol. **222:** 55–70.

O'Connell, K. F., C. Caron, K. R. Kopish, D. D. Hurd, K. J. Kemphues *et al.*, 2001 The *C. elegans zyg-1* gene encodes a regulator of centrosome duplication with distinct maternal and paternal roles in the embryo. Cell **105:** 547–558.

Okuda, M., H. F. Horn, P. Tarapore, Y. Tokuyama, A. G. Smulian *et al.*, 2000 Nucleophosmin/B23 is a target of CDK2/cyclin E in centrosome duplication. Cell **103:** 127–140.

Pelletier, L., N. Ozlu, E. Hannak, C. Cowan, B. Habermann *et al.*, 2004 The *Caenorhabditis elegans* centrosomal protein SPD-2 is

required for both pericentriolar material recruitment and centriole duplication. Curr. Biol. **14:** 863–873.

Sankaran, S., and J. D. Parvin, 2006 Centrosome function in normal and tumor cells. J. Cell Biochem. **99:** 1240–1250.

Simmer, F., C. Moorman, A. M. van der Linden, E. Kuijk, P. V. van den Berghe *et al.*, 2003 Genome-wide RNAi of *C. elegans* using the hypersensitive *rrf-3* strain reveals novel gene functions. PLoS Biol. **1:** E12.

Sluder, G., 2004 Centrosome duplication and it regulation in the higher animal cell, pp. 167–189 in *Centrosomes in Development and Disease*, edited by E. A. Nigg. Wiley-VCH Verlag GmbH, Weinheim, Germany.

Sonnichsen, B., L. B. Koski, A. Walsh, P. Marschall, B. Neumann *et al.*, 2005 Full-genome RNAi profiling of early embryogenesis in *Caenorhabditis elegans*. Nature **434:** 462–469.

Starr, D. A., and J. A. Fischer, 2005 KASH 'n Karry: the KASH domain family of cargo-specific cytoskeletal adaptor proteins. BioEssays **27:** 1136–1146.

Starr, D. A., and M. Han, 2002 Role of ANC-1 in tethering nuclei to the actin cytoskeleton. Science **298:** 406–409.

Timmons, L., and A. Fire, 1998 Specific interference by ingested dsRNA. Nature **395:** 854.

Wang, W., A. Budhu, M. Forgues and X. W. Wang, 2005 Temporal and spatial control of nucleophosmin by the Ran-Crm1 complex in centrosome duplication. Nat. Cell Biol. **7:** 823–830.

Weil, C. F., C. E. Oakley and B. R. Oakley, 1986 Isolation of *mip* (microtubule-interacting protein) mutations of *Aspergillus nidulans*. Mol. Cell. Biol. **6:** 2963–2968.

Wicks, S. R., R. T. Yeh, W. R. Gish, R. H. Waterston and R. H. Plasterk, 2001 Rapid gene mapping in *Caenorhabditis elegans* using a high density polymorphism map. Nat. Genet. **28:** 160–164.

Yoder, J. H., and M. Han, 2001 Cytoplasmic dynein light intermediate chain is required for discrete aspects of mitosis in *Caenorhabditis elegans*. Mol. Biol. Cell **12:** 2921–2933.

Communicating editor: S. Dutcher